Influence of the polymer degradation on enhanced oil recovery processes

Druetta, P.; Picchioni, F.

Published in:
Applied Mathematical Modelling

DOI:
10.1016/j.apm.2018.11.051

Publication date:
2019

Applied Mathematical Modelling 69 (2019) 142–163

Contents lists available at ScienceDirect

Applied Mathematical Modelling

journal homepage: www.elsevier.com/locate/apm

Influence of the polymer degradation on enhanced oil recovery processes

P. Druetta*, F. Picchioni

Department of Chemical Engineering, ENTEG, University of Groningen, Nijenborgh 4, Groningen, 9747AG The Netherlands

ARTICLE INFO

Article history:
Received 15 August 2018
Revised 13 November 2018
Accepted 29 November 2018
Available online 19 December 2018

Keywords:
Enhanced oil recovery
Polymer
Viscoelasticity
Reservoir simulation

ABSTRACT

Polymer flooding is one of the most common and technically developed chemical Enhanced Oil Recovery (EOR) processes. Its main function is to increase the carrying phase's (i.e., water or brine) viscosity in order to mobilize the remaining trapped oil. Many numerical simulators have been developed during the last 30 years considering the influence of the polymer molecules on the viscosity as well as on other physical parameters (e.g., diffusion, adsorption). Nevertheless, there are certain phenomena which were not previously considered, for instance, the interfacial effects of hydrophobically modified polymers. Furthermore, the degradation of the polymer molecules in a harsh environment such as the one found in porous media is well known. This causes a deterioration on the viscosifying properties, diminishing the efficiency of the method. It is important also to consider the effect of the polymer viscoelasticity on the microscopic sweeping efficiency, lowering the residual oil saturation, which has not been properly addressed. A new compositional 2D numerical simulator is presented for polymer flooding in a two-phase, three-component configuration, considering all these physical effects present in porous media and using a fully second-order accurate scheme coupled with total variation diminishing (TVD) functions. Results demonstrated that degradation cannot be considered negligible in any polymer EOR process, since it affected the viscoelastic and viscosifying properties, decreasing the sweeping efficiency at both micro- and macroscopic scales. This simulator will allow setting the desired designing properties for future polymers in relationship with the characteristics of the oil field to be exploited.

1. Introduction

The exploitation of oil and gas fields goes through a number of stages that take advantage of different physical mechanisms in order to mobilize the trapped oil to the producing wells: from an initial, primary recovery stage in which natural mechanisms are used to drive the recovery process, to a secondary stage, when a fluid (e.g., water or CO_2) is injected in order to repressurize the reservoir and sweep the remaining oil from the injectors to the producers. Nevertheless, after these two initial production periods around half of the original oil in place (OOIP) still remains trapped underground. During the last 50 years scientists and companies have developed new, improved techniques as a tertiary stage, known as Enhanced Oil Recovery. During the latter, different sweeping agents are utilized to alter the physical and/or chemical properties of oil,

* Corresponding author.
E-mail address: p.d.druetta@rug.nl (P. Druetta).
URL: http://www.rug.nl/research/product-technology/ (P. Druetta)

https://doi.org/10.1016/j.apm.2018.11.051
0307-904X/

Nomenclature

Ad	component adsorption [day^{-1}]
c_r	rock compressibility [Pa^{-1}]
$\underline{\underline{D}}$	dispersion tensor
dm	molecular diffusion [m^2/s]
dl	longitudinal dispersion [m^2/s]
dt	transversal dispersion [m^2/s]
K	absolute permeability [mD]
K_{MH}	Mark–Houwink constant
k_r	relative permeability
M_w	polymer molecular weight [Da]
p	reservoir pressure [Pa]
p_{wf}	bottomhole pressure [Pa]
q	flowrate [m^3/day]
r_w	well radius [m]
S	phase saturation
s	well skin factor
u	Darcy velocity [m/day]
V	volumetric concentration
z	overall concentration

Greek Letters

α_{MH}	Mark–Houwink constant
δ_{ij}	Kronecker delta
μ	absolute viscosity [Pa·s]
σ	interfacial tension [mN/m]
ϕ	formation porosity
Ω	reservoir domain
Γ	Domain boundary

Superscripts

a	aqueous phase
c	capillary
H	water–oil system (no Chemical)
j	Phase
$< n >$	time-step
o	oleous phase
r	Residual

Subscripts

c	Polymer component
i	Component
in	Injection
m, n	Spatial grid blocks
p	Petroleum component
t	Total
w	Water component

water and/or rock formation in order to mobilize the remaining oil after secondary recoveries, increasing the performance and lifetime of mature oil fields. Of these techniques, one of the most used for low and medium viscosities oil reservoirs is the injection of chemical agents in the water-phase, which is known as CEOR.

1.1. Polymer flooding

Water soluble polymers were one of the first methods developed to increase the efficiency of waterflooding processes, thanks to the pioneering work by Sandiford [1] and Pye [2]. The main objective with the polymer molecules is to alter the rheological properties of the carrying phase (i.e., water/brine), reducing the mobility ratio, which is the relationship between the flowabilities of water and oil phases [1,3–6]. This can be accomplished in two different ways: modifying the rock wettability and/or the phase viscosities. Even though a Newtonian behavior can be adopted for medium and low viscosity oils,

this is not the case for the polymer carrying phase. The solution viscosity depends on, among others, the polymer concentration, architecture and molecular weight, the temperature, water salinity, total dissolved solids (TDS) and the concentration of divalent cations [5]. There is also the discussion whether the polymer may also alter the microscopic efficiency factor, and with this, the residual oil saturation. The results, supported by the literature [7–9], indicate that the viscoelastic and interfacial effects of the polymer molecules affect the latter [5,7–10]. This is therefore taken into account in the development of the new simulator.

However, the polymer flooding process is affected by a number of physical and chemical factors additional to those already known in mass transfer processes which must be taken into account during the simulation. The rheology of the injected solution is one of these key factors. The economic success of the whole process is susceptible to the injection rate, which is directly related to the viscosity of the polymeric solution [11]. The polymer solutions used in the industry have the characteristic of being non-Newtonian, unlike the Newtonian rheology found during the waterflooding. The viscosity depends on the polymer concentration and the shear-rate, which in the case of flow in porous media can reach high values. Nevertheless, while in laboratory tests a shear-thinning behavior has been reported, during flow in porous media, at high shear-rates, a shear-thickening rheology has been found, increasing the viscosity of the solution as the shear-rate increases. This was studied by many authors [5,12] who developed coupled rheological models in order fit the experimental tests. The viscosity depends, through the Flory and Mark–Houwink correlations, on the molecular weight of the polymer, which is a function of the length of the backbone chain. It is known from literature that polymers during flow in porous media are subjected to processes of thermal [13,14], mechanical [15–17], chemical [11,18,19], and/or biological [5,20,21] degradation, which produce a chain-scission of the backbone, affecting negatively the viscosifying properties. In addition to the rheology, the presence of the polymer brings about two phenomena that must be taken into account during the simulation: the permeability reduction of the aqueous phase and the inaccessible pore volume (IAPV). The first is caused by the polymer molecules adsorbed by the rock surface, which resist the flow of the aqueous phase. This can be modeled as an irreversible process reducing the relative permeability of the rock. The second is caused because the polymer molecules, being much larger than water ones, can enter to a limited region of the rock's poral volume. This is modeled as a "reduced pseudo-porosity" that affects only the mass conservation of the chemical component [5,22].

2. Aim of this work

Most commercial and academic simulators do not consider one or more of the important physical phenomena present in polymer EOR flooding, thus the purpose of this research is the development of a new simulator that includes all these phenomena. The model proposed and developed comprises a complete study of degradation due to scission of the backbone chain, which to the extent of our knowledge, has not been reported yet. The degradation process is also a parameter not considered so far in most of simulators. This plays a major role in polymer flooding since the rheological properties are based on the molecular weight. Even though in the literature there are models considering the degradation as mentioned before [23], these are based on models affecting the viscosity itself and not the molecular weight. This approach is not correct since it is not the rheological properties but the molecular structure that is the first parameter affected by the scission of the backbone, and subsequently the radius of gyration, relaxation times, and intrinsic, reduced and zero-shear viscosities.

The first work describing the complete approach using the molecular weight was presented by Lange [24], focusing the study on the thermal degradation process of biopolymers. A thorough analysis of this mechanism was presented, using the Mark–Houwink equation to calculate the zero-shear viscosity based on the molecular weight, using this value in the Carreau–Yasuda viscosity model (which only considers the shear-thinning behavior). Even though this represented a pioneering work in the study of degradation processes in chemical EOR, the mathematical model did not consider the possible shear-thickening effects nor the influence of the biopolymer in the viscoelastic properties of the aqueous phase. Recently, Lohne [25] developed an in-house simulator, IORCoreSim, also taking the approach that the degradation takes place in the molecular weight and therefore affects not only the viscosity. However, this model does not consider the possible influence of the polymer on the interfacial forces. Moreover, even though the effect of degradation on the shear-thickening was considered, its influence on the residual oil saturation due to the viscoelastic nature of the polymer was not modeled. If the viscoelasticity is considered in the model, it must be taken into account that the viscoelastic properties depend on, among others, the relaxation time, which is a function of the molecular structure. Considering the degradation affects only the viscosity and not the viscoelastic properties leaves unaffected a number of parameters related to the viscoelasticity and the residual oil saturation. That is the main reason a complete degradation mechanism is proposed in this new simulator, based on the variation of the molecular weight, hence affecting all the other related properties.

In addition to the previously mentioned physical phenomena, some problems of numerical source have been studied when the mass conservation equation is discretized. To address this issue, a scheme with higher order of convergence was derived, both in time and in space. This scheme has a TVD flux limiting restriction so as to prevent numerical diffusion and dispersion phenomena, and therefore the occurrence of spurious oscillations, commonly found in traditional Finite Difference Method schemes [26]. The combination of the mentioned has resulted in a novel and complete simulator, which can be used for the design and screening of new polymers to be used in EOR.

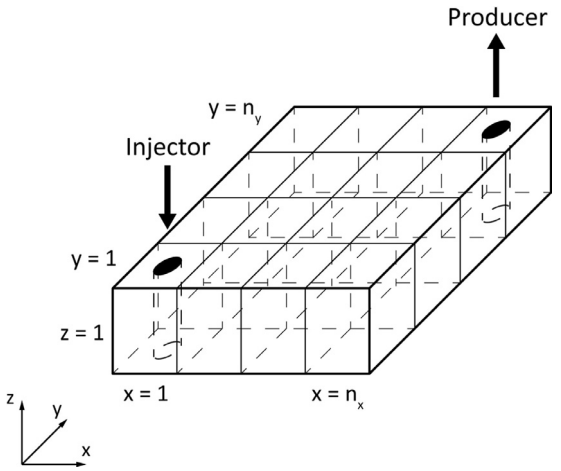

Fig. 1. Schematic representation of the quarter 5-spot used for the simulations [28].

2.1. Physical model

In order to model the process of polymer flooding a 2D geometrical model is used, with a geometric pattern usually found in the oil industry. The five-spot scheme is a good model, consisting of a square domain, with constant or variable properties, where an injection well is placed at the center, and four producing wells are located at the corners. During this analysis, a simplification of the model was performed which known as quarter of five-spot (Fig. 1). The physical model is composed by a reservoir (Ω) of known geometric characteristics, with an absolute permeability (K) and porosity (ϕ), which can be considered constants or to have a statistical distribution. The flow is considered isothermal, incompressible and 2-dimensional (since it is assumed that the vertical permeability is negligible when compared to horizontal ones); it is also considered that the system is in local thermodynamic (phase) equilibrium. The domain is then discretized in a system of $n_x \times n_y$ blocks to perform the numerical simulation. Darcy's law is valid and gravitational forces are negligible compared to the viscous ones [27]. The fluids' rheology behavior can be considered Newtonian or non-Newtonian, depending on the presence of the chemical in the corresponding phase.

Polymer EOR flooding, such as other chemical tertiary oil recovery techniques, involves the flow of fluids in two phases (aqueous and oleous), and various components (water, chemical and petroleum). It is noteworthy that these can be actually mixtures of a number of pure components, since petroleum is a mixture of many hydrocarbons, water contains dissolved salts and the polymer is composed by a number of molecules of different lengths and architectures [11,29,30]. The recovery process involves injecting in a first stage an aqueous solution with the polymer and thereafter a water bank is injected in order to drive the chemical plug, sweeping the mobilized oil into the producing wells. This model is represented by a system of strongly non-linear partial differential equations (PDE) which are completed by a set of algebraic relationships representing physical properties of the fluid and the rock, namely: interfacial tension (IFT), residual phase saturations, relative permeabilities, rock wettability, disproportionate permeability reduction, inaccessible pore volume, phase viscosities, capillary pressure, adsorption on the formation, and dispersion.

2.2. Mathematical model

In the particular case of CEOR processes, the physical and chemical properties of the phases present in the reservoir depend on the concentration of the components, rendering a strongly non-linear system and thus traditional numerical approaches (e.g., *black-oil* model) are not suitable. The compositional flow approach on the other hand allows the simulation of a multiphase, multicomponent system in which all the properties can be expressed as functions of the concentrations. This numerical model is based originally on a first-order compositional simulator developed also for EOR flooding [28], which was validated against commercial and academic simulators in a series of 2D flooding processes. Subsequently, this simulator was improved using a second-order TVD scheme, validating its results and furthermore its order of accuracy in secondary and tertiary recovery processes [31]. Since this model is an extension of a previous, validated one, it is considered that the validation process previously done is valid for this new model [32–34]. Hence, the Darcy, mass conservation and aqueous pressure equations yield,

$$\vec{u}^j = -\underline{\underline{K}} \cdot \frac{k_r^j}{\mu^j} \cdot \vec{\nabla} p^j;\ j = o, a \tag{1}$$

$$\frac{\partial(\phi z_i)}{\partial t} + \nabla \cdot \sum_j V_i^j \cdot \vec{u}^j - \nabla \cdot \sum_j \underline{\underline{D_i^j}} \cdot \nabla \cdot V_i^j = -\frac{\partial \phi A d_i}{\partial t} + q_i;\ i = p, c, w \tag{2}$$

$$\underline{\underline{D_i^j}} = dm_i^j \cdot \phi \cdot S^j \cdot \delta_{ij} + \|\vec{u}^j\| \cdot \left[\frac{dl^j}{\|\vec{u}^j\|^2} \cdot \begin{pmatrix} (u_x^j)^2 & u_x^j \cdot u_y^j \\ u_y^j \cdot u_x^j & (u_y^j)^2 \end{pmatrix} + dt^j \cdot \begin{pmatrix} 1 - \frac{(u_x^j)^2}{\|\vec{u}^j\|^2} & -\frac{u_x^j \cdot u_y^j}{\|\vec{u}^j\|^2} \\ -\frac{u_y^j \cdot u_x^j}{\|\vec{u}^j\|^2} & 1 - \frac{(u_y^j)^2}{\|\vec{u}^j\|^2} \end{pmatrix} \right] \tag{3}$$

$$\phi c_r \frac{\partial p^a}{\partial t} + \vec{\nabla} \cdot (\lambda \cdot \nabla p^a) = \frac{\partial}{\partial t}\left(\phi \cdot \sum_i Ad_i\right) - \vec{\nabla} \cdot (\lambda^o \cdot \nabla p_c) + q_t \tag{4}$$

The aim of the polymer in the displacing phase (i.e., water) is to increase its viscosity and therefore reduce the mobility ratio, avoiding the formation of viscous fingering in the reservoir which decreases the macroscopic sweeping efficiency [4,5,10,35]. Along with this, we also consider the influence of several well-known phenomena in the process, such as the physical diffusion of the polymer in the aqueous phase, and the adsorption of the polymer molecules onto the rock formation. These are well-documented aspects of polymer flooding, which have already been taken into account in previous simulators [25,36–43]. However, in this model a modification of the latter is proposed in several aspects which, to our understanding, should be present in any polymer chemical flooding simulator. The most important is the degradation of the polymer molecules in the reservoir. The harsh conditions (i.e., thermal, mechanical and chemical) present in underground media subject the polymer to a degradation process [5,11,13–21], in which the scission of the chains causes a detriment in the viscosifying properties. In this new simulator this is considered by including an extra differential equation modeling the average molecular weight as a function of time (see Section 3.5). Furthermore, it is known from the literature [7–10] that the viscoelastic properties of polymer solutions create an extra stress condition which is responsible of increasing the microscopic sweeping efficiency and thus, decreasing the residual oil saturation. This must also be considered and expressed as a function of the polymer molecular weight. Moreover, the simulator also allows for the possibility of carrying out flooding processes with hydrophobically modified polymers, which are also known for lowering the interfacial energy between oleous and aqueous phases [44]. A simple formulation to take into account the possible presence of these groups in the polymer backbone, which affects ultimately the capillary number, is proposed and discussed.

3. Physical properties

3.1. Chemical component partition

The most important part of a numerical simulation using a compositional model is to understand how the components distribute into the phase, which is called phase behavior of the system. The component partition in polymer flooding is relatively simple, since it is assumed that the oleous phase is purely composed of the petroleum component present in the system. Therefore, water and chemical components are only present in the aqueous phase. This is represented in Eq. (5) by the volumetric concentrations of petroleum, polymer and water in the oleous phase. With these relationships the system becomes numerically determined with a unique solution, and the parameters previously introduced can be calculated for each representative elementary volume (REV).

$$V_p^o = 1 \wedge V_c^o = V_w^o = 0 \tag{5}$$

3.2. Interfacial tension

The interfacial tension of the water–oil system depends on the presence and concentration of the polymer in the porous media. However, the effect of the polymer on the IFT is not the most important in the whole process and it is not as effective as in the case of surfactant flooding. Most importantly, the influence of the polymer depends also on its structure. When the latter is fully soluble in water, such as HPAM, the polymer does not influence the water–oil interfacial properties [45,46]. However, when the polymer molecule has hydrophobic groups distributed along the backbone, these will affect the IFT and lower the interfacial energy [44,47,48]. In order to model the influence of these hydrophobically modified polymers, a simple correlation is introduced based on the work presented by Wever [49] and Pancharoen [50], in which the IFT varies approximately in a linear way between two values of the polymer concentration, from a maximum value σ_{ow} to its minimum constant value for higher concentration of polymer (Fig. 2). The reduction of IFT allows mobilizing the oil trapped in the reservoir and its influence is measured by the capillary number.

3.3. Residual saturation

The relationship between the velocity field, the interfacial energy and the residual oil saturation can be described by means of the capillary number N_{vc}. From this dimensionless group it becomes clear the importance of both the interfacial tension and the displacing phase viscosity. A piecewise function allows obtaining the residual saturation for wetting and non-wetting phases.

$$N_{vc} = \frac{u \cdot K}{\lambda \cdot \sigma} \tag{6}$$

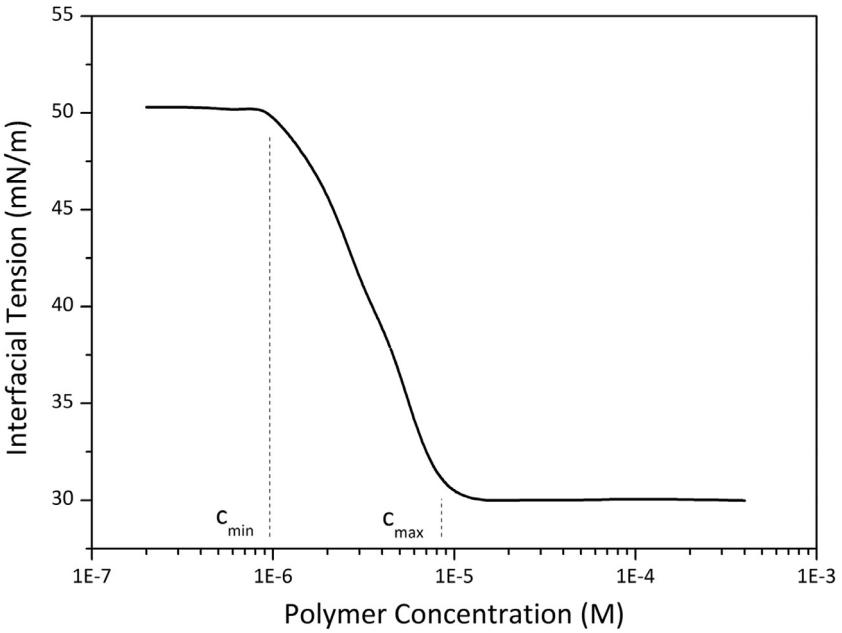

Fig. 2. Adopted model of the IFT as a function of polymer concentration (Based on Wever[49]).

$$\frac{S^{jr}}{SjrH} = \begin{cases} 1 & \textbf{if} \quad N_{vc} < 10^{\left(\frac{1}{T_1^j}\right)-T_2^j} \\ T_1^j \cdot [\log(N_{vc}) + T_2^j] & \textbf{if} \quad 10^{\left(\frac{1}{T_1^j}\right)-T_2^j} \leq N_{vc} \leq 10^{-T_2^j} \\ 0 & \textbf{if} \quad N_{vc} > 10^{-T_2^j} \end{cases} \tag{7}$$

However, several authors discussed on how the viscoelastic properties of polymer solutions influence the residual oil viscosity, and this is not only evidenced in the shear-thickening region polymer solutions develop at high shear-rates, but also in the microscopic sweeping efficiency [6]. It is because of this reason that it is proposed in this paper to make a modification to Eq. (7) in order to take into account the effects of viscoelasticity in the polymer solution. With that purpose, when this equation is applied for the aqueous phase, the factor T_2^o is considered as a function of a parameter which takes into account the shear rate and the viscoelastic properties of the polymer (Eq. (8)). The Weissenberg number (Wi) relates to both phenomena and it is therefore the factor modifying T_2^o (Eq. (9)).

$$T_{2,mod}^o = T_2^o \cdot \left(1 + T_2^{o,v} V_c^a Wi^n\right) \tag{8}$$

$$Wi = \lambda \frac{u^a}{L} \tag{9}$$

$$\lambda = \frac{6M_w(\mu_{0sr} - \mu_{water})}{\pi^2 R_g V_c^a T} \tag{10}$$

where λ is the polymer relaxation time, R_g is the universal gas constant, T is the field temperature, and n and $T_2^{o,v}$ are constants to fit the experimental data. This is calculated according to the radius of gyration, which is a function of the molecular weight. With this parameter the effects of the viscoelasticity can be quantified in typical oil/water desaturation curves (Fig. 3). The oleous line is then displaced to the left, decreasing the normalized residual oil saturation for the same N_{vc}. In waterflooding processes the relaxation time of the water molecules is negligible, thus the oleous desaturation curve is not affected. When a polymer solution is injected, the viscoelasticity shifts the desaturation curve to the left, causing the oleous phase to be desaturated at lower capillary numbers [51]. Moreover, the relaxation time is a function of the molecular weight, so in order to fully couple the numerical model with the degradation process the relationship between both factors is taken into account (Eq. (10)) [7–10,51,52]. This, to our best understanding, is the first time a model takes into account the degradation process to a full extent, with molecular weight, relaxation time, desaturation curves, and relative permeabilities varying as a function of time.

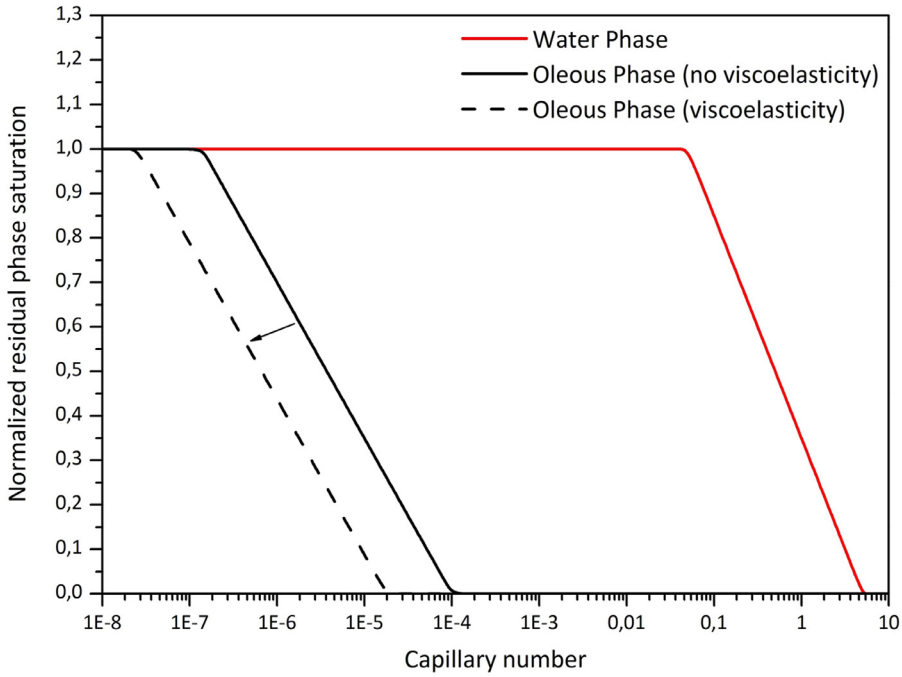

Fig. 3. Capillary desaturation curves for non-wetting (oleous) and wetting (aqueous) phases, showing the influence of the new model on the oleous residual saturation.

3.4. Inaccessible pore volume

This phenomenon was first reported by Dawson and Lantz [53], who noticed that polymer molecules traveled faster than other chemical species in water phase. This is due to the size of the polymer molecules which cannot penetrate in the entire poral volume, whereas other small molecules (e.g. water, tracers) can access the whole domain. This is then influenced by the size and architecture of the polymer and the physical properties of the porous medium. The purpose of this parameter (IAPV) is then to compensate this process causing the polymer flow to be faster than the other components. Since then, several authors have confirmed this phenomenon in laboratory-scale experiments [54–56]. This is quantified in the polymer mass conservation (Eq. (2)) where an extra-term is added affecting the porosity [22].

$$\phi_{IAPV} = 1 - \frac{IAPV}{\phi} \wedge \phi_{i=c} = \phi \cdot \phi_{IAPV} \tag{11}$$

3.5. Phase viscosities

Much has been written about the rheological characteristics of polymer solutions. They present a non-Newtonian behavior with a shear-thinning profile in rheometry experiments [57,58]. The most used correlations to describe this are the Power-Law (or Ostwald–de Waele) and the Carreau–Yasuda Law. Three different zones can be distinguished (Fig. 4), namely: the upper Newtonian where the viscosity remains somewhat constant and similar to the zero-shear viscosity; then, a shear-thinning region similar to the one described by the Power Law; and finally the lower Newtonian region at high shear rates where the viscosity is similar to the pure solvent viscosity. However, it has been reported that the rheological behavior of polymer solution is different in porous media, where shear rates can reach high values. At low- and medium-shear rates the solution has the same behavior as in the experiments. But after a critical value, a shear-thickening behavior is observed [41]. This is also called extensional flow, and the viscosity is described as the sum of the shear-thinning and the extensional (or elastic) viscosity. This phenomenon is caused by the elasticity of polymer molecules. It is noteworthy to mention that at even higher shear rates a maximum viscosity is achieved followed by a gradual decrease. This is due to the mechanical degradation phenomenon when the polymer chains are ruptured by the fluid acceleration field, lowering the molecular weight and the viscosity.

The first step in modeling the rheology of the solution is to adopt a model that allows quantification and evaluation of both phenomena. The Unified Viscosity Model (UVM) developed by Delshad [12] is a correlation used and validated for the entire range of shear rates encountered in porous media. The overall viscosity (μ_{UVM}) consists of two terms, the shear-thinning viscosity (μ_{ST}), dominant at low and medium shear-rates, and the elastic viscosity (μ_{ELAS}) which becomes

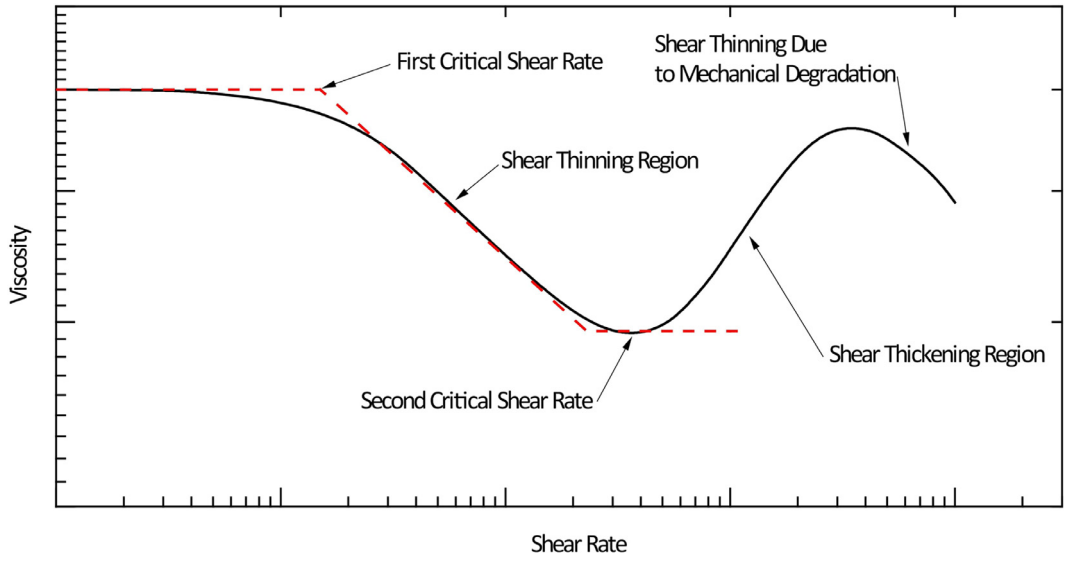

Fig. 4. Rheological model used in the simulation (UVM) compared to the Carreau–Yasuda regions.

important as the shear rate increases (Fig. 4). The shear thinning term is expressed according to the Carreau relationship,

$$\mu_{UVM} = \mu_{ST} + \mu_{ELAS} \tag{12}$$

$$\mu_{ST} = \mu_{0sr} + (\mu_w - \mu_{0sr}) \cdot \left[1 + \left(\frac{\dot{\gamma}}{\tau_r}\right)^2\right]^{\left(\frac{n-1}{2}\right)} \tag{13}$$

$$\mu_{ELAS} = \mu_{MAX} \cdot \left[1 - e^{-(\lambda_2 \tau_2 \dot{\gamma})^{n_2 - 1}}\right] \tag{14}$$

where μ_{0sr} is the viscosity of the solution at zero shear-rate, μ_w is the viscosity of water, $\dot{\gamma}$ is the shear rate, and β_1, β_2 and n are input parameters according to the rheological behavior, which defines the first critical shear rate, where the fluid passes from the upper Newtonian regime to the shear thinning region. The elastic viscosity is defined as,

$$\tau_r = \beta_1 \cdot e^{\beta_2 V_c^a} \tag{15}$$

$$\tau_2 = \tau_0 + \tau_1 \cdot V_c^a \tag{16}$$

$$\mu_{MAX} = \mu_w (AP_{11} + AP_{22} \cdot \ln V_c^a) \tag{17}$$

where λ_2, n_2, τ_0, τ_1, AP_{11}, AP_{22} are the input parameters of the shear thickening region. The main concern for this formulation is then to find a way to calculate or measure the critical parameters, namely: μ_{MAX} and μ_{0sr}. For instance, Wang [52] suggested using a function to relate the elastic and the shear thinning viscosities. This approach will be followed in the model to express the critical parameters, accepting that the maximum shear thickening viscosity will be a function of the zero shear viscosity. The problem then has been reduced to finding a proper relationship for the zero shear viscosity [57,59]. The modified Flory equation [60] is adopted to calculate this viscosity,

$$\mu_{0sr} = \mu_w \left[1 + \left(AP_1 V_c^a + AP_2 V_c^{a^2} + AP_3 V_c^{a^3}\right) C_{SEP}^{Sp}\right] \tag{18}$$

the term C_{SEP}^{Sp} takes into account the dependence of the polymer viscosity on the salinity and the percentage of divalent cations in the latter present in the porous medium. This can be written as the specific viscosity, and the terms expressed as functions of the intrinsic viscosity as follows:

$$\mu_{sp} = \left(AP_1 V_c^a + AP_2 V_c^{a^2} + AP_3 V_c^{a^3}\right) C_{SEP}^{Sp} \tag{19}$$

The AP_i parameters are expressed as a function of the intrinsic viscosity,

$$AP_1 = k_1 \cdot [\eta]; AP_2 = k_2 \cdot [\eta]^2; AP_3 = k_3 \cdot [\eta]^3 \tag{20}$$

where k_i are constants obtained from laboratory experiments or rheology measurements affecting the specific viscosity. Finally, the intrinsic viscosity can be related to the average molecular weight using the Mark–Houwink formula,

$$[\eta] = K_{MH} \cdot M_w^{\alpha_{MH}} \tag{21}$$

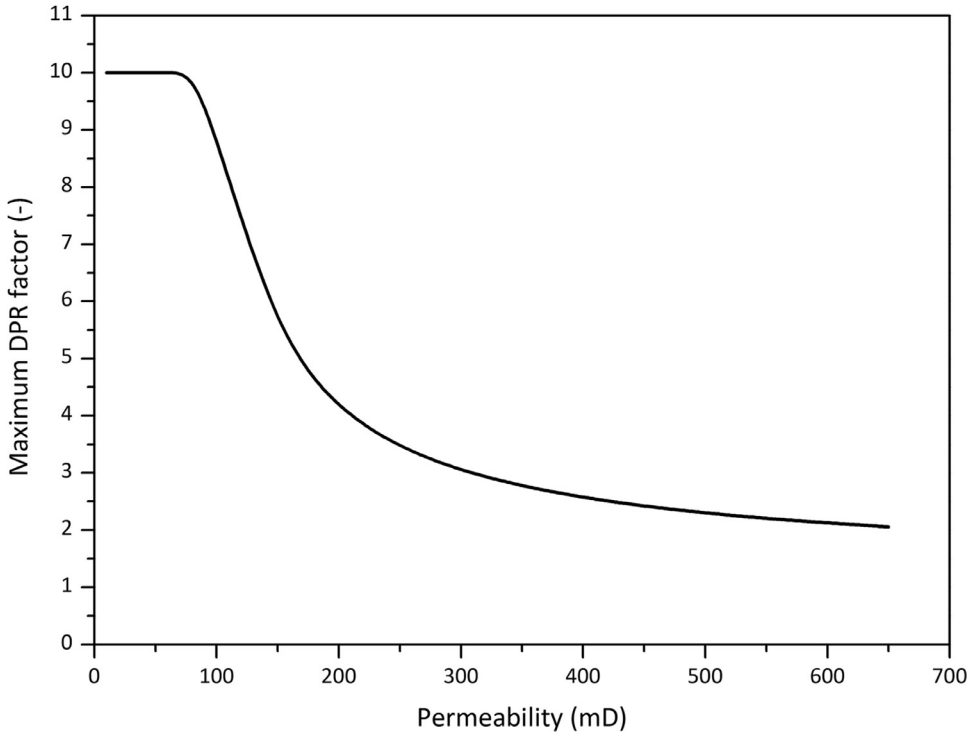

Fig. 5. Maximum DPR factor as a function of the absolute permeability.

A relationship between the rheological behavior of the polymer solution and the molecular weight has been reached which, to our best knowledge, has never been proposed in polymer simulators in the literature. It is well documented that polymer solutions undergo several degradation mechanisms in underground porous media, namely: mechanical (due to high shear rates), chemical (due to the presence of salts), thermal (related to high temperature reservoirs), and biological (bacteria affecting mostly biopolymers)[13–21]. These mechanisms cannot be excluded when longer flooding processes are being performed. The problem consists then in understanding how the polymer degrades as a function of the time it remains underground. This degradation will cause the scission of the backbone chain, modifying the molecular weight and therefore the rheological properties. In order to simulate the degradation, an exponential decay law will be assumed in the average molecular weight. This law was selected based on degradation experiments presented in the literature as well as numerical models developed to consider the degradation of polymer chains in porous media [61–66]. This yields,

$$\frac{dM_w}{dt} = -\lambda_{degmec} M_w \tag{22}$$

The degradation parameter (λ_{degmec}) will regulate how fast the (macro)molecules degrade and the molecular weight decreases with time. For the purpose of this simulation, the decay parameter will be considered constant. However, this depends on many factors according to the mechanisms involved and the polymers used. For instance, the salinity or bacteria concentration are not constant throughout the whole domain, and these values affect seriously the degradation rate.

For the oil phase, since it was assumed that no water or chemical are present in the phase, the rheology behavior can be considered as that of the pure oil. According to the literature [3,11,22,29], light and medium oil cuts exhibit Newtonian behavior while heavy oil might present a slight shear-thinning rheology [67]. For the purpose of this simulator, the oleous phase will be considered as a Newtonian fluid.

3.6. Disproportionate permeability reduction

As a result of the adsorption process, polymer molecules in the rock will resist the flow of the aqueous phase, which can interpreted as a decrease in the relative permeability function. This phenomenon is called disproportionate permeability reduction (DPR) or relative permeability modification (RPM). There is a direct relationship between the adsorbed molecules and the permeability reduction. This is an irreversible process, since the DPR does not decrease if the polymer concentration does, and it can be used as an indicator for the degree of channel blocking in the porous media. Then, the DPR factor can

Table 1
Reservoir geometrical and initial parameters.

Geometrical data of the reservoir					
Length in axis X	500 m	Length in axis Y	500 m	Layer thickness	5 m
n_x	25 elements	n_y	25 elements		
Rock properties					
Porosity	0.25	k_{xx}	200 mD	k_{yy}	200 mD
Initial conditions					
S_o	0.70	S_o^r (EOR)	0.35	$S_a^{rH} = S_o^{rH}$	0.15
Simulation data					
Total time	5000 days	Chem. injection time	200 days	z_{clN}	0.025
Physical data of the phases					
μ^{aH}	1 cP	μ^{oH}	20 cP	Oil density	850 kg/m^3
Water density	1020 kg/m^3	IFT	50 mN/m		

Table 2
Wells operating conditions.

Physical data					
Number of wells	2	Well radius	0.25 m	Skin factor	0
Operating conditions					
Total flowrate	1650 STB/day	Bottomhole pressure	55,160 kPa		

be modeled as [5,22,68,69],

$$R_k = 1 + \frac{(R_{k,max} - 1) b_{rk} V_c^a}{1 + b_{rk} V_c^a} \tag{23}$$

where $R_{k,\,max}$ is the maximum permeability reduction factor and b_{rk} is an input parameter related with the adsorption process. This value can be obtained from core experiments or according to the following expression [5,22,52]:

$$R_{k,max} = \min \left\{ \left[1 - \frac{c_{rk} \left(A P_1 C_{SEP}^{Sp} \right)^{\frac{1}{3}}}{\left(\frac{\sqrt{K_x K_y}}{\phi} \right)^{\frac{1}{2}}} \right]^{-4}, R_{k,cut} \right\} \tag{24}$$

where c_{rk} is an input parameters related to the physical properties of the porous medium and the salinity present in the domain. The empirically-determined term $R_{k,\,cut}$ is used as the upper limit of DPR and set in the simulator to a value of 10, although factors higher than this value were reported in low permeability fields (Fig. 5) [5,70].

4. Results and discussion

4.1. Introduction

It has been observed that after secondary recovery processes a minimum amount of oil is still flowing out, with a significant amount of oil still trapped. However, values produced are below an economically limiting threshold, rendering the exploitation not profitable. This limit is known as minimum operating flow. The latter does not have a certain fixed value, depending on the country, the region and the dynamic economic factors. To mobilize the remaining oil tertiary recovery processes are employed. For this type of process the non-iterative method cannot be used, since the resulting system of equations is strongly non-linear.

Then, a polymer flooding will initially be simulated in an oil field with initial conditions similar to the waterflooding. It is expected that, due to the better mobility ratio, the time employed in the process will be significantly lower than the time used in the waterflooding. After an initial period with an aqueous polymer solution being injected, a water bank follows in order to drive the polymer slug towards the producing well.

4.1.1. Data

As it was done in a previous paper [28], a series of properties are established aimed at emulating a EOR recovery process in an low-viscosity oil reservoir (Tables 1 and 2).

4.2. Influence of the degradation rate

The polymer molecules used in EOR processes suffer from different types of degradation, which cannot be ignored or overridden. They produce, due to various sources, a break in the main backbone chain, resulting in a decrease of viscosifying

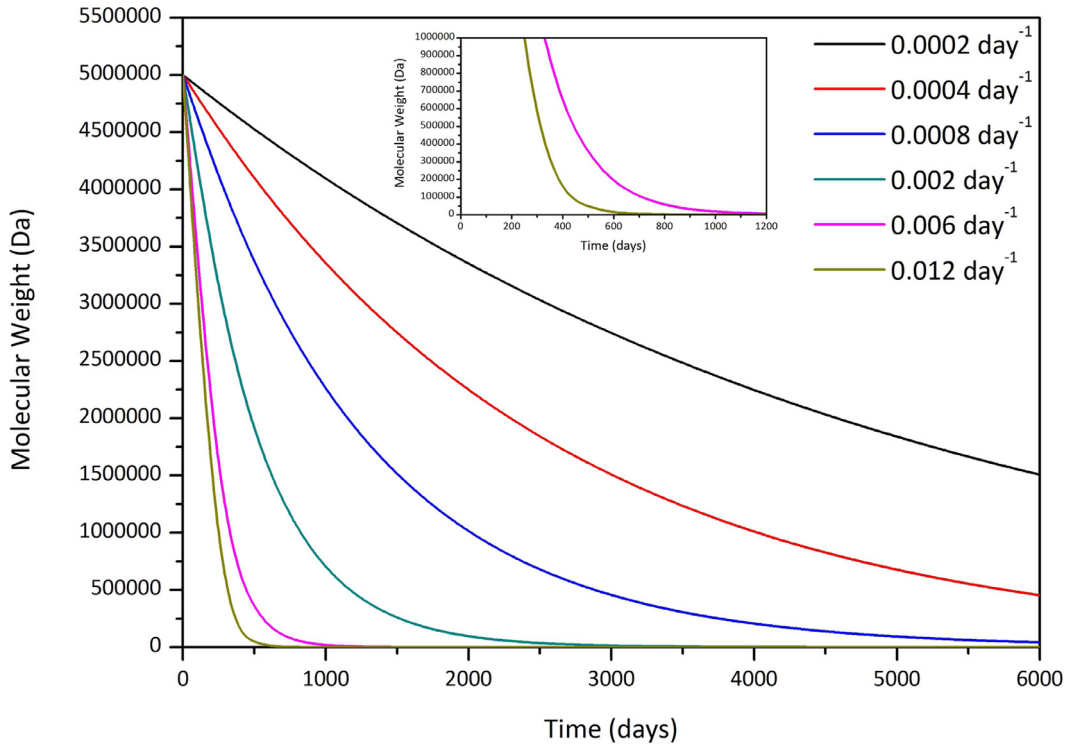

Fig. 6. Degradation rates (λ_{degmec}) and their influence on the polymer average molecular weight (degradation rates based on Wang [52]).

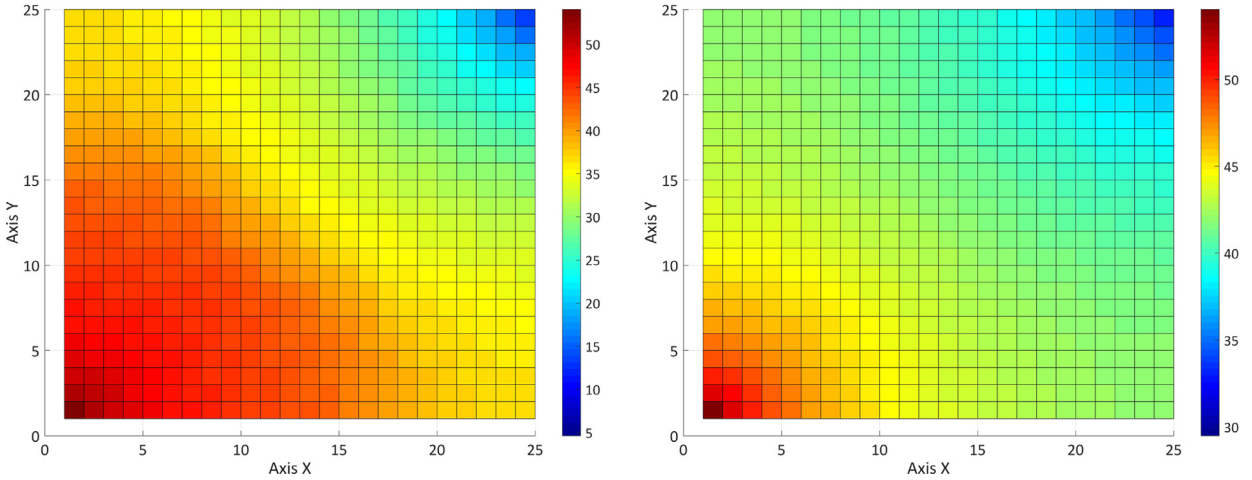

Fig. 7. Pressure field [MPa] after 750 days (left) and 5000 days (right) for a degradation rate of 2×10^{-4} day^{-1}.

properties and also affecting the viscoelastic behavior of the solution through the relaxation time (Eq. (10)). Simulations performed mimic different degrees of degradation that may be associated with the presence of salts, bacteria, temperature, and/or demanding operating conditions. The first part of this section studies the influence of the degradation in a porous medium of constant properties, and then the same procedure is applied in a heterogeneous medium. In this study six different degradation rates are studied affecting the polymer's average molecular weight, which were selected to compare the results with those found in the literature (Fig. 6) [52].

The results of the simulations are presented in Figs. 7 to 9. As was anticipated, increasing degradation rates affect negatively the sweeping process since they increase the mobility ratio, which means the aqueous phase will flow easier than the trapped oil. The values obtained matched those from the literature: for lower degradation rates (< 0.001 day^{-1}) the sweeping efficiency of the polymer renders still higher values than those from waterflooding [52]. However, as the former exceeds 0.01 day^{-1}, the values tend to be those obtained in standard waterflooding, since the polymer loses its viscosifying

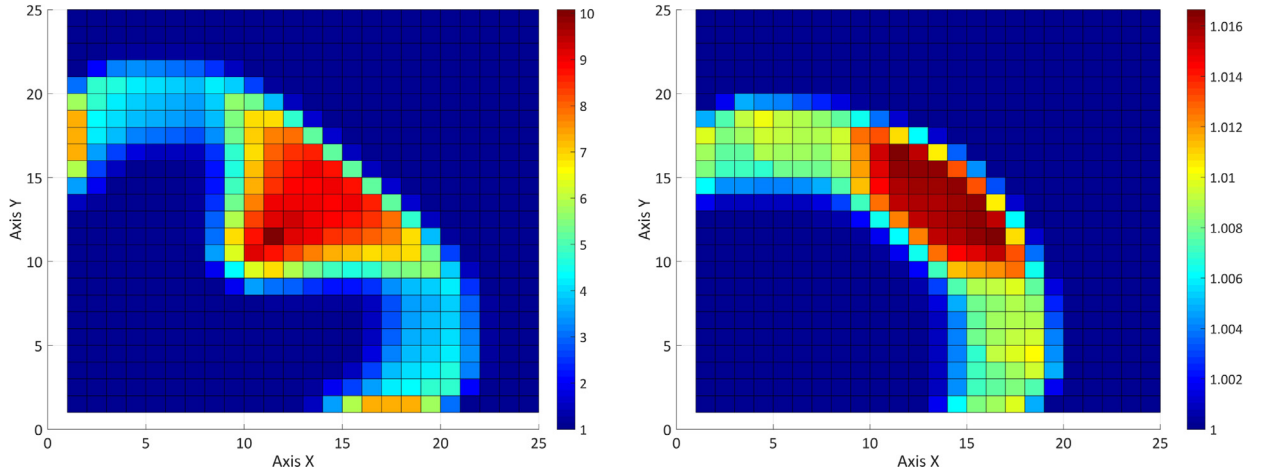

Fig. 8. Aqueous phase viscosity [mPa·s] after 1000 days for a degradation rate of 2×10^{-4} (left) and 12×10^{-3} (right) day^{-1}.

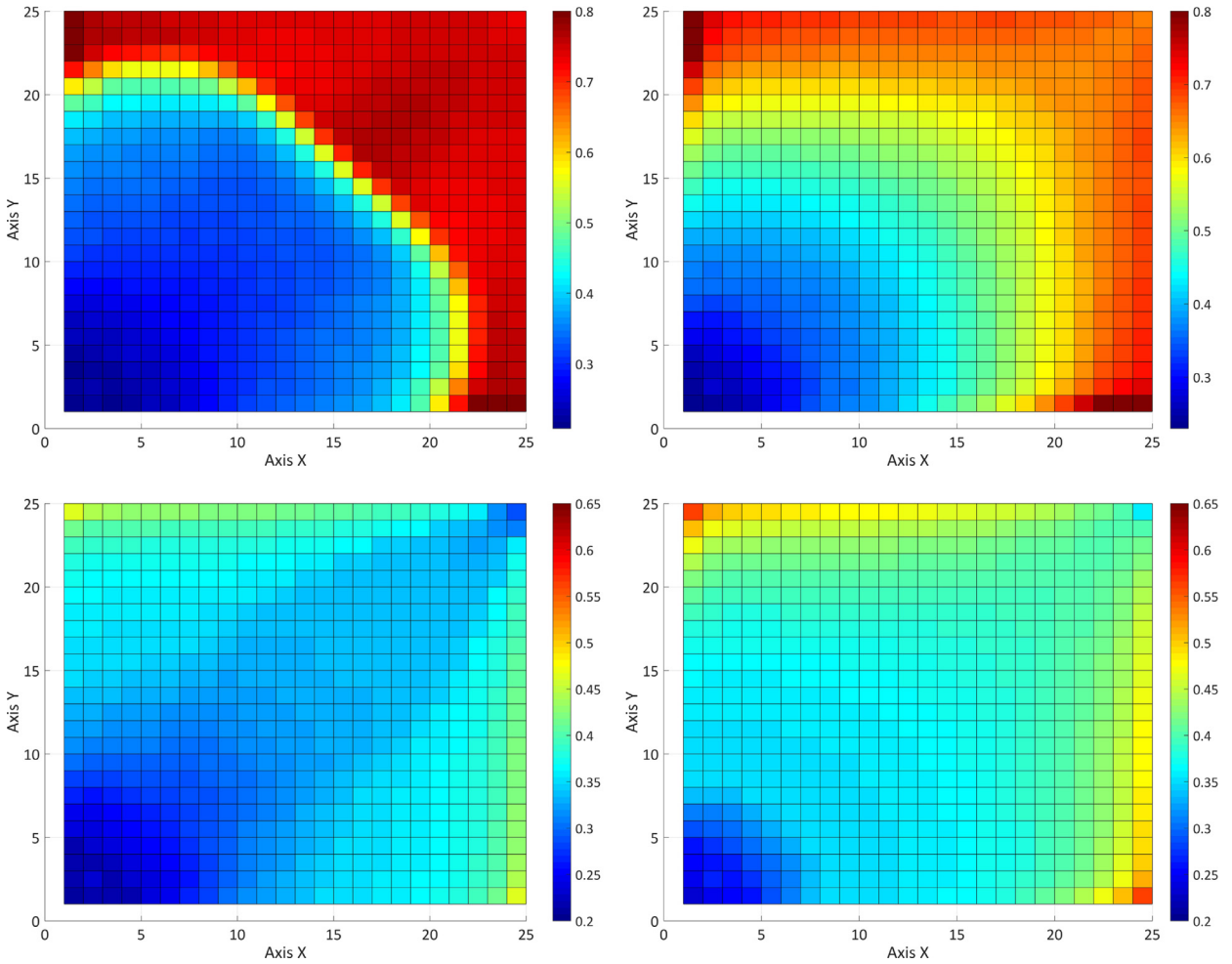

Fig. 9. Oil saturation profiles after 1000 days (top) and 5000 (bottom) days, for degradation rates of 2×10^{-4} (left) and 12×10^{-3} (right) day^{-1}.

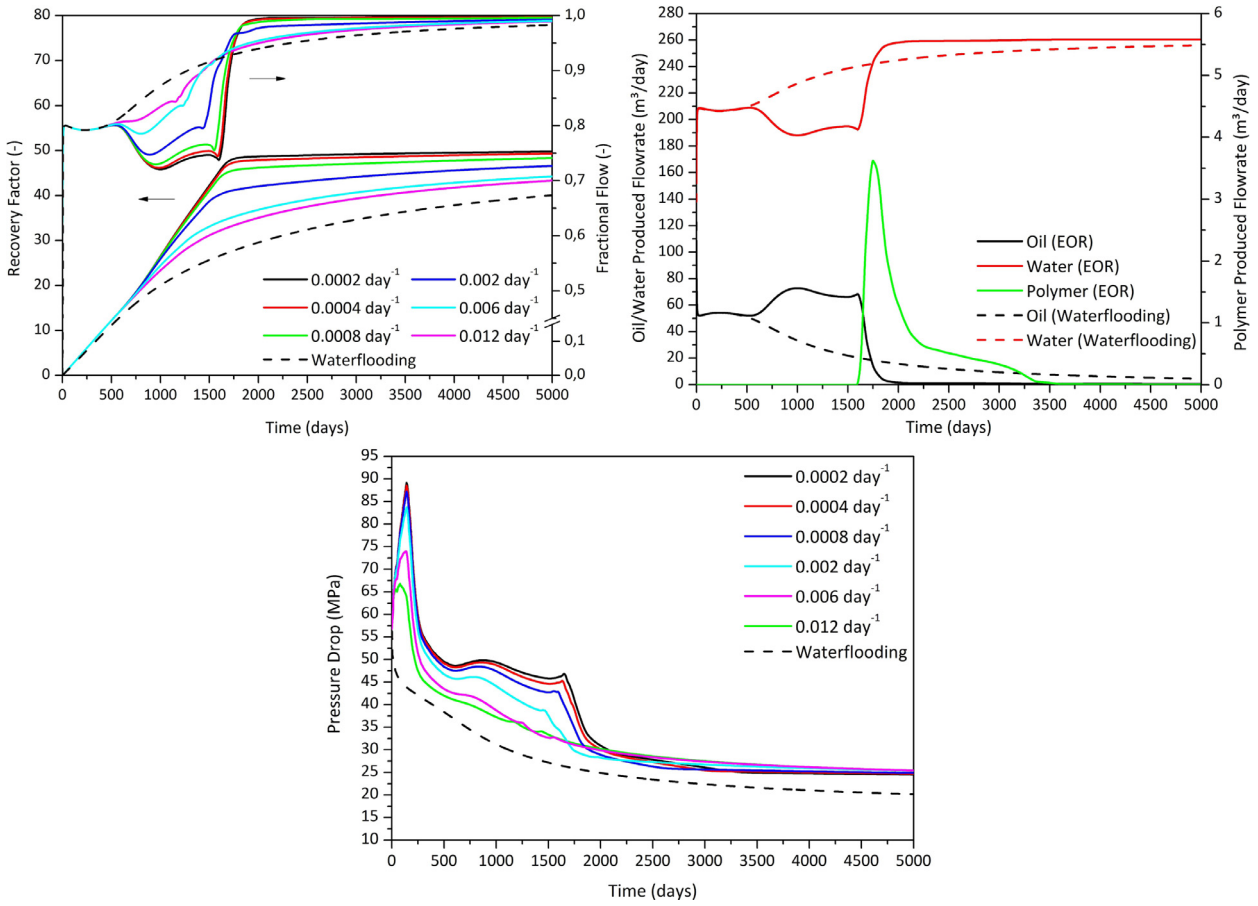

Fig. 10. Cumulative oil production and fractional flow (top left), oleous/aqueous/polymer produced flowrates for the case with degradation 2×10^{-4} day^{-1} (top right), and pressure drop (bottom) for different degradation rates in a polymer EOR flooding.

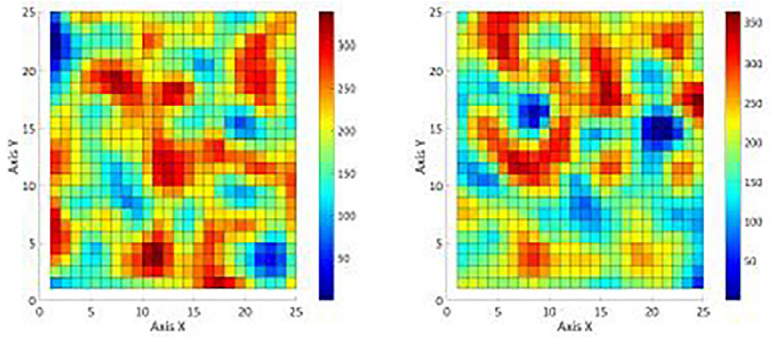

Fig. 11. Permeability field (in mD) used to study the influence of the oil viscosity in the simulator.

properties after a short period of time (Fig. 8). It is noteworthy to mention that in Fig. 7, even though the viscosity profiles for the minimum and maximum degradation rates are similar, their maximum values differ significantly: while for the case with 2×10^{-4} day^{-1} the maximum aqueous phase viscosity is 10 mPa·s (left), for the case with the maximum degradation rate (12×10^{-3} day^{-1}) the maximum viscosity is slightly above the water's (1.016 mPa·s - right).

It is noteworthy to analyze in Fig. 8 the shape of the polymer solution as a function of the degradation rate. This is due to a physical process and it is not generated by possible numerical effects due to the grid orientation [71]. When the later is high (Fig. 8 - right) the fluid tends to behave as a quasi Newtonian fluid with values approximately similar to those from the water/brine. However, at low degradation rates (Fig. 8 - left), the influence of the polymer renders a non-Newtonian fluid. Thus, the pressure gradient affects the shear-rate, which has a more notorious influence on the phase viscosity (and on the phase mobility), modifying the polymer transport properties.

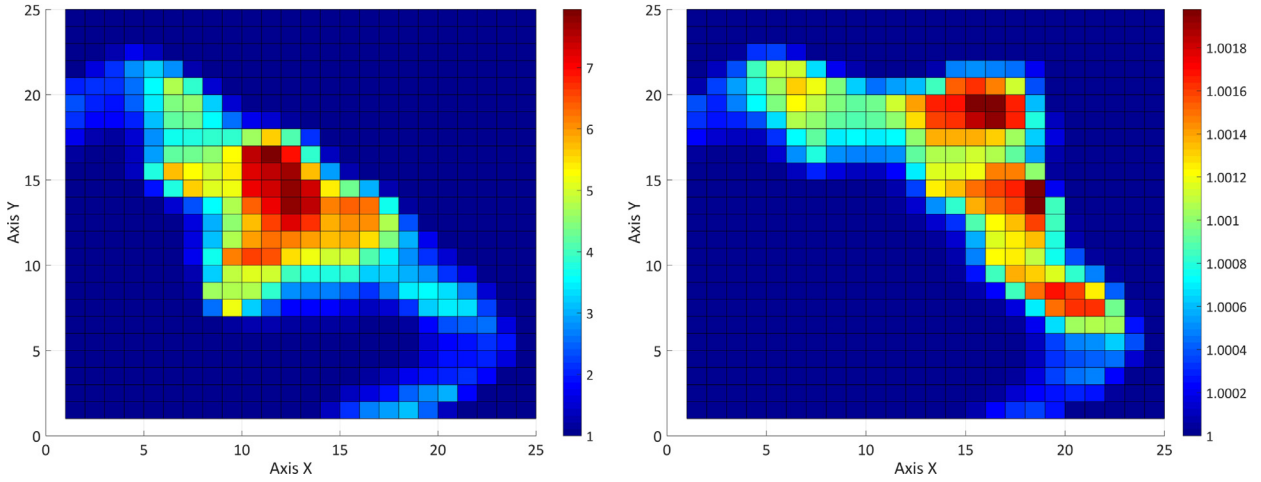

Fig. 12. Aqueous phase viscosity [mPa·s] after 1000 days in a random permeability field for a degradation rate of 2×10^{-4} (left) and 12×10^{-3} (right) day^{-1}.

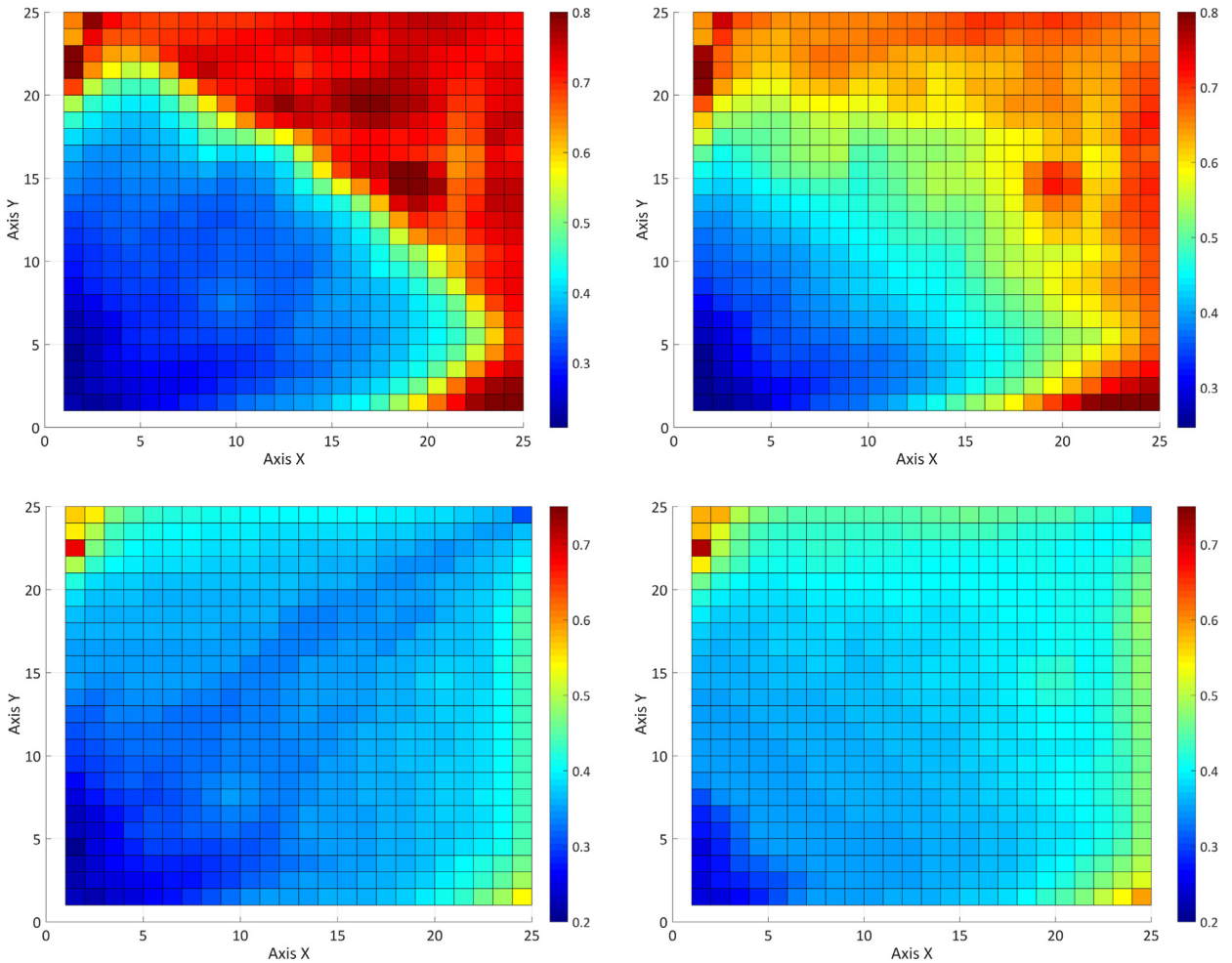

Fig. 13. Oil saturation profiles after 1000 days (top) and 5000 (bottom) days in a heterogeneous field for degradation rates of 2×10^{-4} (left) and 12×10^{-3} (right) day^{-1}. See the Appendix for the interactive 3D images of the simulations.

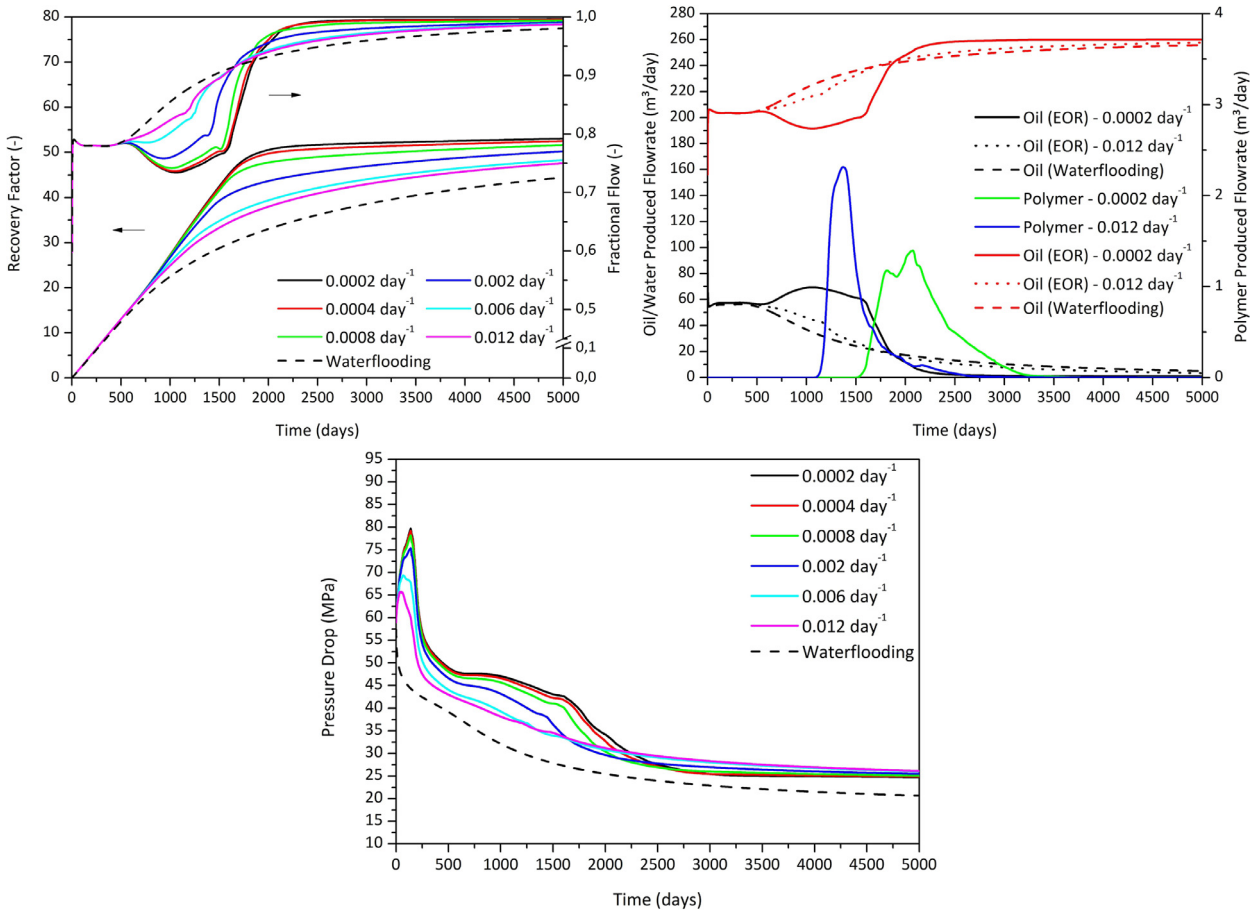

Fig. 14. Cumulative oil production and fractional flow (top left), oleous/aqueous/polymer produced flowrates for the case with degradation rates 2×10^{-4} and 12×10^{-3} day^{-1} (top right), and pressure drop (bottom) for different degradation rates in chemical EOR flooding in a heterogeneous oil field.

Fig. 9 depicts the oil saturation profiles at different stages for two degradation rates (λ_{degmec}). In the case with low degradation, the polymer sweeps efficiently the oil with a uniform wave front (Fig. 9 - left), and the chemical breakthrough takes place approximately 1600 days after the simulation started, reaching the economic threshold for the fractional flow 200 days after the case with a greater degradation rate. Moreover, the total recovery factor is higher than in the case of waterflooding with a significant lower time employed to achieve this value. Furthermore, near the wells, a partial desaturation (below the waterflooding residual saturation) was achieved due to the viscosifying and elastic properties of the polymer solution, which was inversely proportional to the degradation rate. The overall performance of the processes with respect to the simulation time is shown in Fig. 10.

As foreseen, higher degradation rates provoked a decreasing of the sweeping efficiency, which is observed as an increase of the minimum fractional flow during the simulation and higher times employed to attain similar recovery factors. The pressure drop also was significantly affected, with an initial increase due to the polymer slug being injected in the oil field and then a steady decrease followed by a sudden drop after the polymer and oil breakthroughs. The maximum peak depends on the degradation rate as well as the time when these breakthroughs take place, the faster the polymer degrades, the faster the breakthrough will occur. In Fig. 10 it is also observed that the final pressure drop in the polymer cases is slightly higher than the waterflooding final pressure drop. This is due to the DPR, which it is an irreversible process causing a decrease in the flowability of the aqueous phase.

Subsequently the influence of the degradation rate in a heterogeneous porous medium is presented, in order to analyze possible differences or similarities with the previous study. As in the case of waterflooding, a heterogeneous field was generated in MATLAB (Fig. 11) maintaining the same number of numerical cells (or REV's) as in the case of a homogeneous EOR process.

The influence of the heterogeneous permeability field is observed in Figs. 12 and 13. The wave of the polymer slug is deformed due to the difference in the flowability of each node, changing the shear rate and therefore the viscosity. Regarding the oil saturation profile, the case with lower degradation rate is less susceptible to the heterogeneities of the medium and the flooding process behaves as in the previous case. However, when degradation rates increase and polymer solution starts

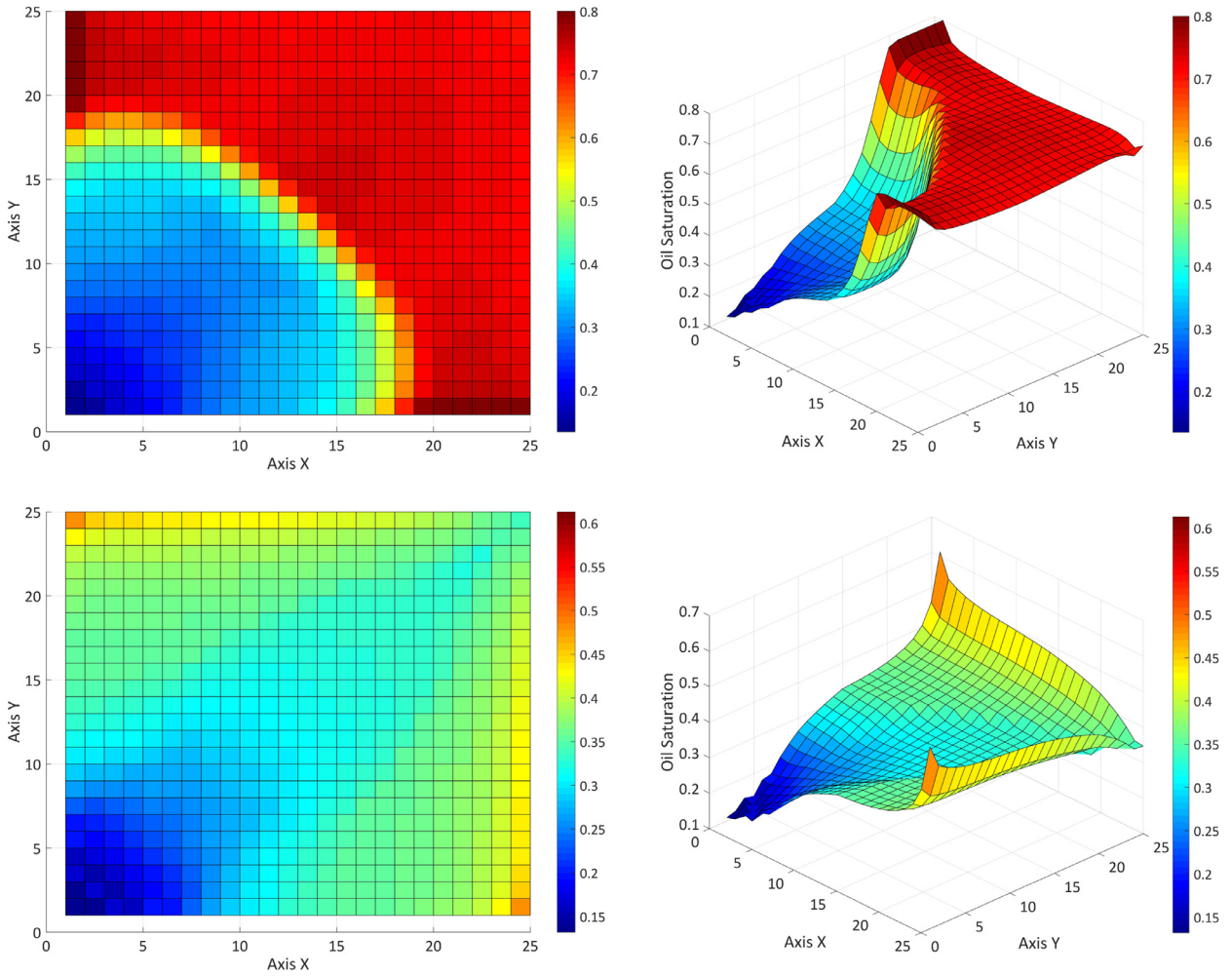

Fig. 15. Oil saturation profiles after 750 (top) and 5000 (bottom) days, taking into account the influence of the viscoelasticity in the residual oil saturation.

behaving like a waterflooding process, the influence of these heterogeneities become more important, with a phenomenon similar to viscous fingering appearing in the front wave (Fig. 13).

The behavior is similar to the previous case, with slight differences of the recovery percentages under different degradation rates (Fig. 14). The latter makes the chemical breakthrough occur faster, due to the fact that a viscosity-decreasing polymer solution displaces to the producing well without sweeping the remaining oil, which is the reason why the fractional flow does not decrease substantially in cases with higher degradation rates.

4.3. Influence of viscoelasticity on the residual saturation

It is well known from the literature [7–10] that polymer solutions present viscoelastic properties. These have proved numerically and experimentally to decrease the residual oil saturation below the values obtained with rheologically-similar solutions, but without exhibiting viscoelasticity [52]. The new model takes into account this in the oil residual desaturation curves. The influence of such property was based on a dimensionless group, the Weissenberg number, which takes into account both the viscoelastic properties caused by the polymer molecules and the shear-rate in the porous media. This number is affected by the degradation present in the field since the relaxation time is dependent on the molecular weight which, as previously studied, is steadily decreasing as result of degradation phenomena. The results of the simulation and its comparison with non-viscoelastic solutions are presented in Figs. 15 and 16.

The new model did not affect the front wave of the polymer slug, which was expected. However, it is evident from Fig. 15 that the residual oil saturation near the injection went below the values obtained for non-viscoelastic solutions (Fig. 9). This is mainly due to a combined mechanism of high shear-rate near the well and a relaxation time which it was not yet affected by the degradation process. In the rest of the field a similar trend to a non-viscoelastic polymer flooding is observed. Nevertheless, it is clear from Fig. 15 (bottom right) that a channel-shaped region occurred between the wells,

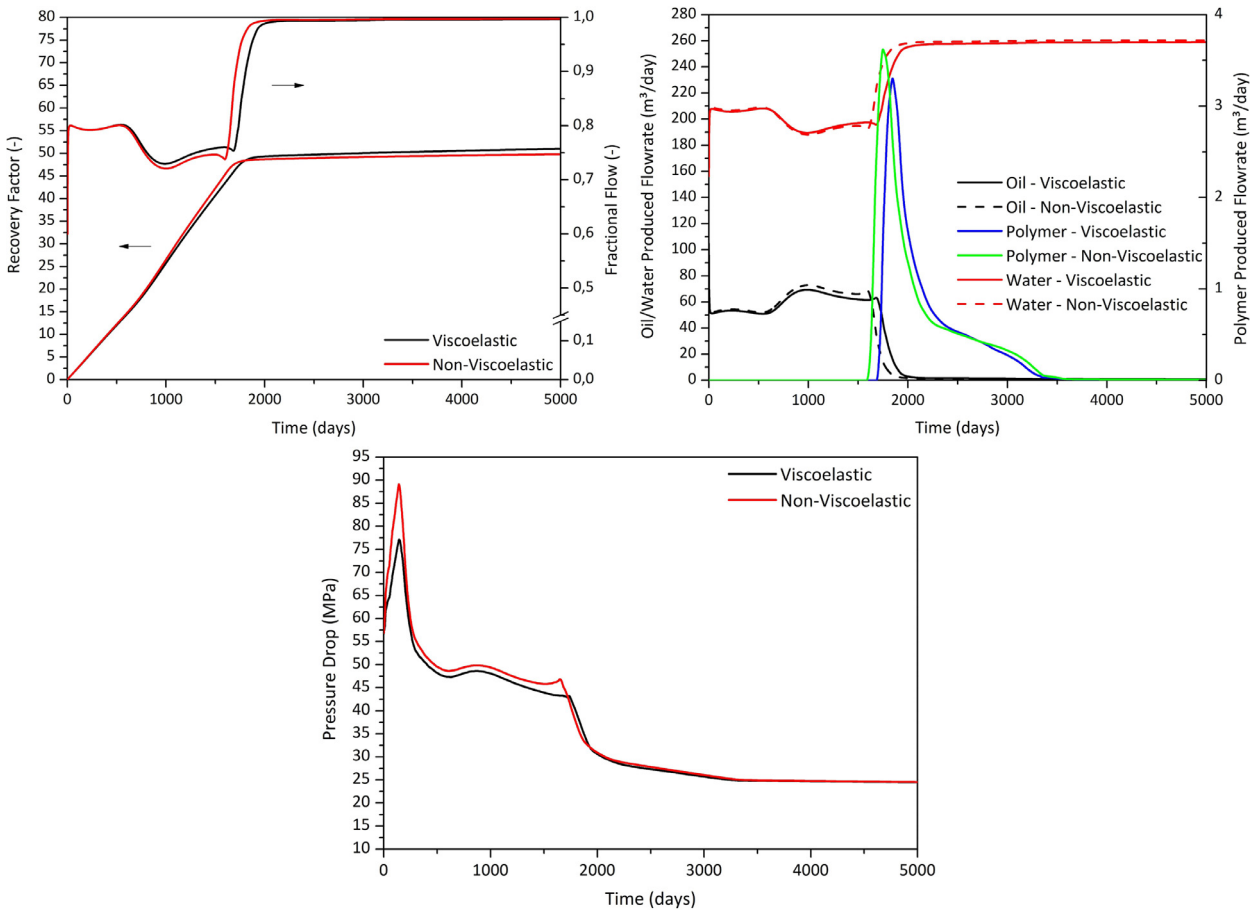

Fig. 16. Cumulative oil production and fractional flow (top left), oleous/aqueous/polymer produced flowrates (top right); and pressure drop (bottom) for a chemical viscoelastic/non-viscoelastic EOR flooding.

with residual saturations below waterflooding. This trend corresponds also with results found by Wang [52]. The overall performance of the process is shown in Fig. 16. The sweeping efficiency with a viscoelastic fluid follows a similar behavior to the observed in previous cases. However, the enhanced sweeping efficiency is seen in the extended low-fractional flow period, which increased the recovery factor. This caused the polymer slug breakthrough to be delayed with respect to the non-viscoelastic case (Fig. 16 - middle). The pressure peak during the viscoelastic flooding was observed to be lower than in previous cases, which can be related to the fact that oil relative permeability was affected by the oil desaturation curve, and the former modified the pressure field when solving Eq. (1). However, when the polymer slug became negligible in the oil field, the pressure drop difference between viscoelastic and non-viscoelastic became imperceptible.

4.4. Waterflooding and Polymer flooding combined

A comprehensive analysis of a polymer EOR flooding has been discussed along with the influence of the different numerical and physical factors. As a final part of this paper, a combined operation of water- and polymer flooding is performed. As a common strategy in oilfields [3,11], after the primary recovery a waterflooding takes place until the economic threshold of the fractional flow (f_a) is achieved. This can be defined as the ratio between the aqueous and the total flowrate at the producing wells and it is usually employed as a critical parameter to determine the profitability of a recovery process. Then, EOR techniques follow in order to enhance the exploitation performance of the oil field. However, this approach can be optimized by introducing the EOR process before this limit is reached, as has been already mentioned in the literature [5]. Therefore, in order to study this influence, a previous waterflooding was carried out in the oil field and final values for different water cuts in the production well were stored as a starting point for EOR operations. The results are presented in Figs. 17 to 19. As reported in the literature [3,5], the faster the polymer flooding starts, the better the efficiency of the whole process is (Fig. 20). This is due to the fact that a considerable time is necessary for waterflooding to reach this limit value, with a minimum extra oil recovery. Starting EOR flooding at lower values of water cuts decreases the time employed, and therefore, the operational costs (Fig. 20 - left).

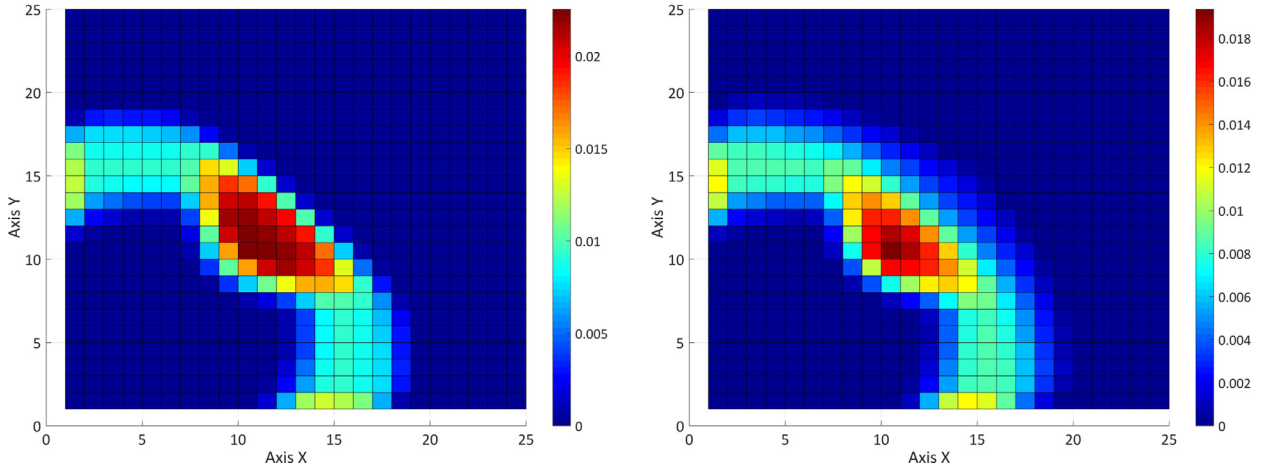

Fig. 17. Polymer concentration after 750 days of EOR operations for the combined case with $f_a = 0.85$ (left - 1590 days after start of operations) and $f_a = 0.98$ (right - 5300 days after start of operations).

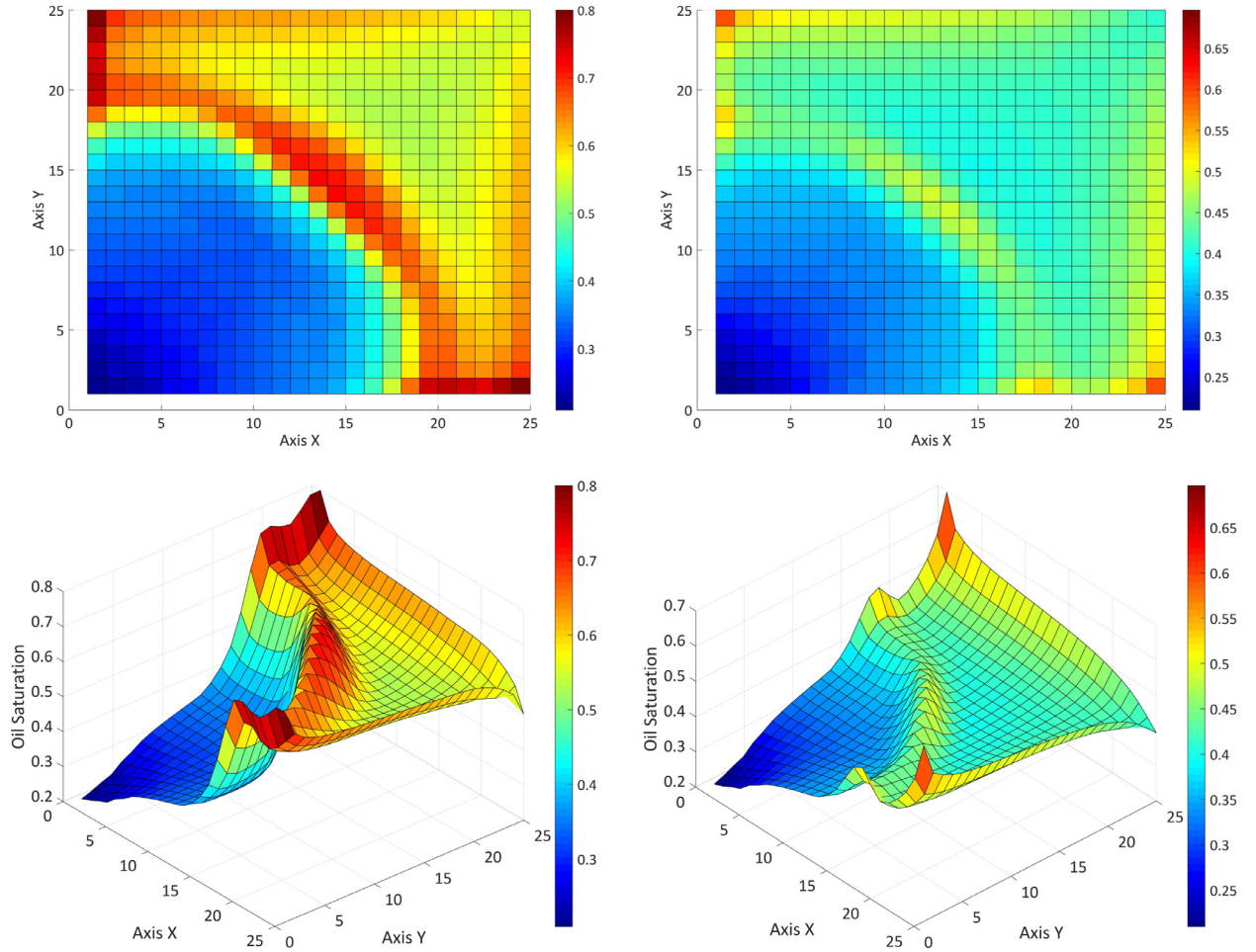

Fig. 18. Oil saturation profiles after 750 days of EOR flooding, for the combined case with $f_a = 0.85$ (left - 1,590 days after start of operations) and $f_a = 0.98$ (right - 5300 days after start of operations). See the Appendix for the interactive 3D images of the simulations.

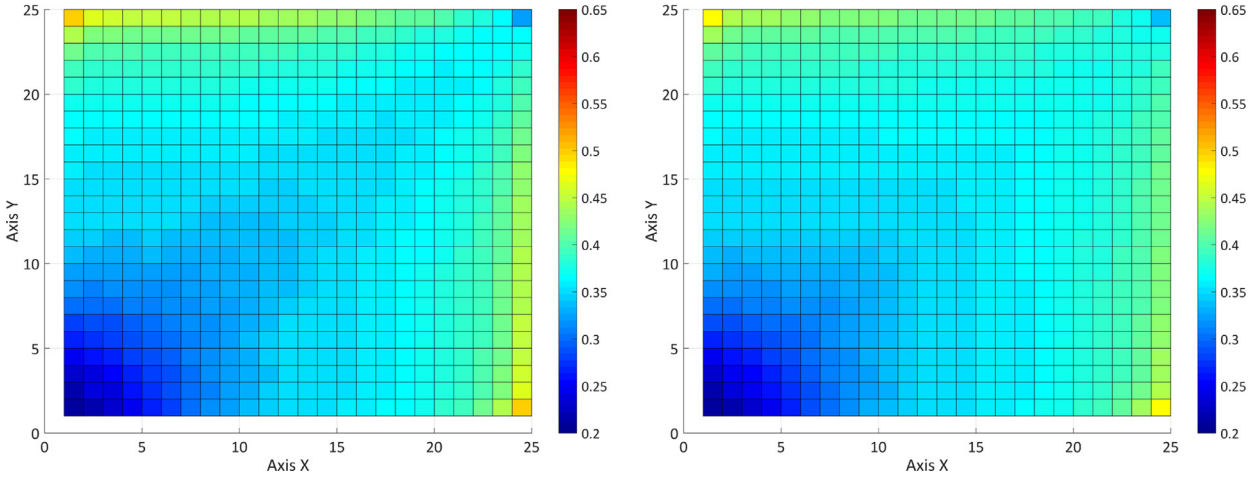

Fig. 19. Final oil saturation profiles after 5000 days of EOR flooding, for the combined case with $f_a = 0.85$ (left - 5840 days after start of operations) and $f_a = 0.98$ (right - 9550 days after start of operations).

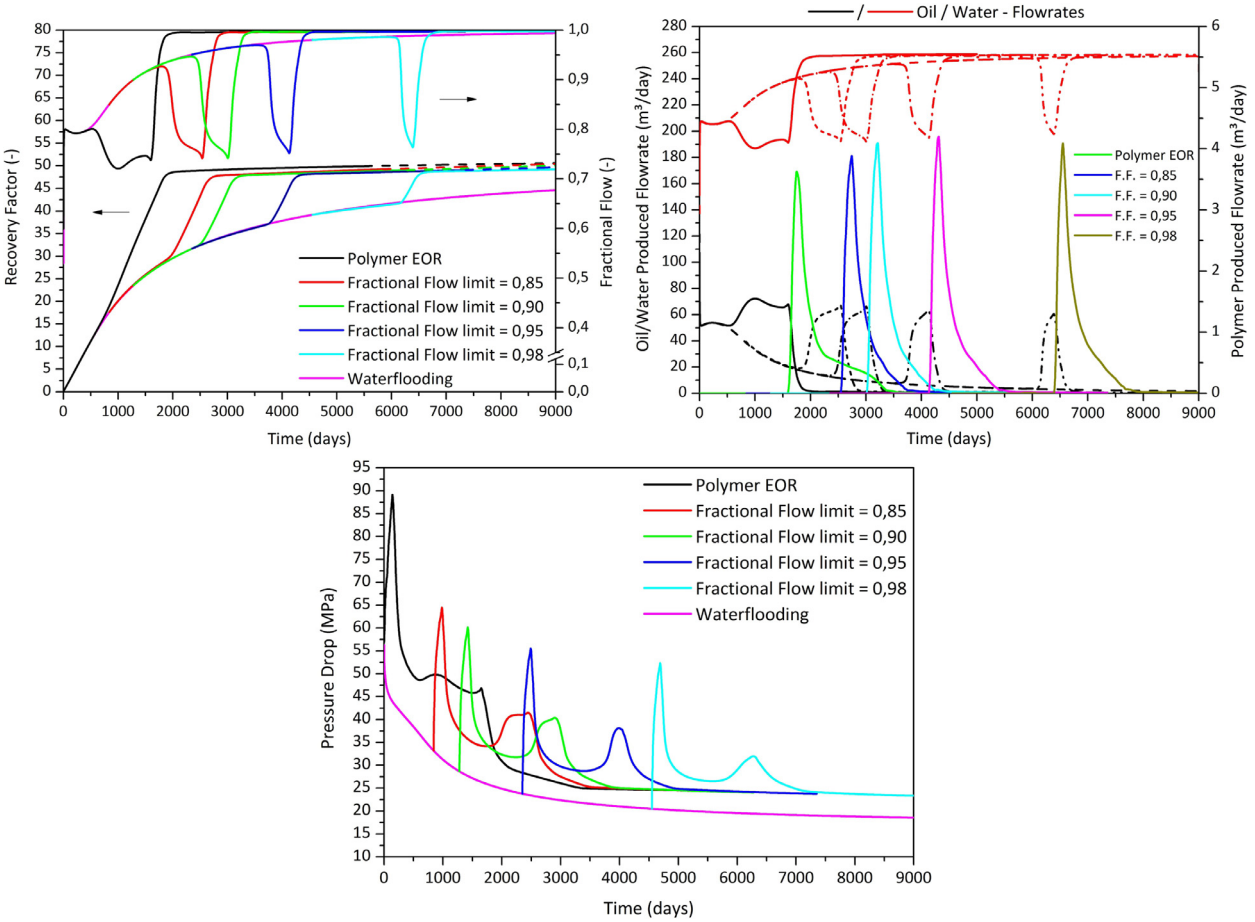

Fig. 20. Cumulative oil production and fractional flow (top left), oleous/aqueous/polymer produced flowrates (top right) and pressure drop (bottom) for a chemical EOR/waterflooding combined flooding process.

Figs. 18 and 19 show the result of the combined process for the different strategies, including the base cases, waterflooding and polymer EOR flooding. As it was mentioned, the earlier EOR operations start, the higher oil recoveries will be, and shorter times will be employed to attain these values, lowering the cost of the overall investment (Fig. 20). However, a drawback of this strategy is the increasing pressure drop, as shown in Fig. 20 (right). When an EOR flooding alone is performed the pressure drop during polymer injection reaches higher values than combined strategies, which can cause problems in the surface facilities. When a previous waterflooding is carried out, the maximum pressure achieved is lowered decreasing the difference between extreme values, which represents a positive aspect for the design of injection facilities.

5. Conclusions

This paper aimed at presenting the application of a novel numerical simulator to a polymer flooding process. The multiphase, multicomponent model takes into account all the important physical parameters present in a chemical flooding and moreover, it includes novel mathematical formulations for significant parameters in the process, such as the degradation rate and the polymer viscoelasticity. Furthermore, the use of a simulator which allows modeling all the conditions to which the polymer is submitted is vital for the development and synthesis of new products resistant to a harsh environment.

Although there are simulators that take into account these factors, a new mathematical formulation has been developed here to study the degradation process from the point of view of molecular weight. Furthermore, since the residual saturations are functions of the viscoelastic properties of oil, the desaturation curves were modified to account for this phenomenon. The fundamental contribution of the model is that the viscoelastic properties depend on the relaxation time, which in turn is a function of molecular weight. A new correlation was introduced to account for the phenomenon of degradation in the relaxation time, and therefore in the desaturation curves, which to the extent of our knowledge, has never been published in the literature. The new desaturation model considering the viscoelastic properties modified the residual oil saturation profile after the polymer flooding, and this also depended on the degradation rate. This new model allows considering the viscoelasticity from two different perspectives: the shear-thickening phenomenon and the development of a new stress field, affecting the parameters of the residual desaturation curves.

The study of the aforementioned properties is essential to model processes that resemble the results in laboratory and field tests. Consequently, a comprehensive study of them should be mandatory during synthesis and application of new macromolecules for polymer EOR. The new simulator allows performing a complete study of degradation depending on the model chosen, which is a function of several parameters prevailing in the porous medium. A correct choice of the degradation model is then essential to make an accurate simulation of polymer flooding process.

Acknowledgments

P.D. gratefully acknowledges the support of the Erasmus Mundus EURICA scholarship program (Program number 2013-2587/001-001-EMA2) and the Roberto Rocca Education Program.

Supplementary material

Supplementary material associated with this article can be found, in the online version, at doi:10.1016/j.apm.2018.11.051.

References

[1] B.B. Sandiford, Laboratory and field studies of water floods using polymer solutions to increase oil recoveries, J. Pet. Technol. 16 (8) (1964) 917–922, doi:10.2118/844-PA.
[2] D.J. Pye, Improved secondary recovery by control of water mobility, J. Pet. Technol. 16 (8) (1964) 911–916, doi:10.2118/845-PA.
[3] E.C. Donaldson, G.V. Chilingarian, T.F. Yen, Enhanced Oil Recovery, I: Fundamentals and Analyses, Elsevier Science, Amsterdam, the Netherlands, 1985. ISBN 978-0-08086-872-1.
[4] R.S. Seright, M. Seheult, T. Talashek, Injectivity characteristics of EOR polymers, SPE Reserv. Eval. Eng. 12 (5) (2009) 783–792.
[5] J. Sheng, Modern Chemical Enhanced Oil Recovery, Elsevier, Amsterdam, the Netherlands, 2011. ISBN 0-08-096163-0; 978-0-08096-163-7.
[6] D.G. Wreath, A Study of Polymer Flooding and Residual Oil Saturation, University of Texas at Austin, USA, 1989.
[7] D. Wang, G. Wang, W. Wu, H. Xia, H. Yin, The influence of viscoelasticity on displacement efficiency - from micro to macro scale, in: SPE Annual Technical Conference and Exhibition, Society of Petroleum Engineers, 2007, doi:10.2118/109016-MS.
[8] D. Wang, H. Xia, S. Yang, G. Wang, The influence of visco-elasticity on microforces and displacement efficiency in pores, cores and in the field, in: SPE EOR Conference at Oil & Gas West Asia, Society of Petroleum Engineers, 2010, doi:10.2118/127453-MS.
[9] B. Wei, L. Romero-Zerón, D. Rodrigue, Mechanical properties and flow behavior of polymers for enhanced oil recovery, J. Macromol. Sci. Part B 53 (4) (2014) 625–644, doi:10.1080/00222348.2013.857546.
[10] Z. Lijuan, Y. Xiang'an, G. Fenqiao, Micro-mechanisms of residual oil mobilization by viscoelastic fluids, Pet. Sci. 5 (1) (2008) 56–61, doi:10.1007/s12182-008-0009-1.
[11] L.W. Lake, Enhanced Oil Recovery, Prentice-Hall Inc., Englewood Cliffs, USA, 1989. ISBN 0-13-281601-6.
[12] M. Delshad, D.H. Kim, O.A. Magbagbeola, C. Huh, G.A. Pope, F. Tarahhom, Mechanistic interpretation and utilization of viscoselastic behavior of polymer solutions for improved polymer-flood efficiency, in: SPE Symposium on Improved Oil Recovery, Society of Petroleum Engineers, 2008, doi:10.2118/113620-MS.
[13] J.J. Maurer, G.D. Harvey, Thermal degradation characteristics of poly(acrylamide-co-acrylic acid) and poly(acrylamide-co-sodium acrylate) copolymers, Thermochim. Acta 121 (0) (1987) 295–306, doi:10.1016/0040-6031(87)80180-6.
[14] H. Al-Sharji, A. Zaitoun, G. Dupuis, A. Al-Hashmi, R. Al-maamari, Mechanical and thermal stability of polyacrylamide-based microgel products for EOR, in: SPE International Symposium on Oilfield Chemistry, Society of Petroleum Engineers, 2013, doi:10.2118/164135-MS.
[15] C. Booth, The mechanical degradation of polymers, Polymer 4 (0) (1963) 471–478, doi:10.1016/0032-3861(63)90060-0.

[16] J.F. Argillier, A. Dupas, R. Tabary, I. Henaut, P. Poulain, D. Rousseau, T. Aubry, Impact of polymer mechanical degradation on shear and extensional viscosities: toward better injectivity forecasts in polymer flooding operations, in: SPE International Symposium on Oilfield Chemistry, Society of Petroleum Engineers, 2013, doi:10.2118/164083-MS.
[17] R. Farinato, W. Yen, Polymer degradation in porous-media flow, J. Appl. Polym. Sci. 33 (7) (1987) 2353–2368, doi:10.1002/app.1987.070330708.
[18] R.D. Shupe, Chemical-stability of polyacrylamide polymers, J. Pet. Technol. 33 (8) (1981) 1513–1529, doi:10.2118/9299-PA.
[19] H. Kheradmand, J. François, V. Plazanet, Hydrolysis of polyacrylamide and acrylic acid-acrylamide copolymers at neutral ph and high temperature, Polymer 29 (5) (1988) 860–870, doi:10.1016/0032-3861(88)90145-0.
[20] M. Bao, Q. Chen, Y. Li, G. Jiang, Biodegradation of partially hydrolyzed polyacrylamide by bacteria isolated from production water after polymer flooding in an oil field, J. Hazard. Mater. 184 (1) (2010) 105–110, doi:10.1016/j.jhazmat.2010.08.011.
[21] M. Fang, W. Li, The molecular biology identification of a hydrolyzed polycrylamide (HPAM) degrading bacreria strain h5 and biodegradation product analysis, in: Proceedings of the International Conference on Environmental Science and Technology, 2007, pp. 135–141.
[22] M. Delshad, G. Pope, K. Sepehrnoori, UTCHEM Version 9.0 Technical Documentation, Center for Petroleum and Geosystems Engineering, The University of Texas at Austin, USA 78751.
[23] J. Wang, H.Q. Liu, J. Xu, Mechanistic simulation studies on viscous-elastic polymer flooding in petroleum reservoirs, J. Dispers. Sci. Technol. 34 (3) (2013) 417–426, doi:10.1080/01932691.2012.660780.
[24] E.A. Lange, C. Huh, A polymer thermal decomposition model and its application in chemical EOR process simulation, in: SPE/DOE Improved Oil Recovery Symposium, Society of Petroleum Engineers, 1994, doi:10.2118/27822-MS.
[25] A. Lohne, O. Nodland, A. Stavland, A. Hiorth, A model for non-newtonian flow in porous media at different flow regimes, Comput. Geosci. 21 (5-6) (2017) 1289–1312, doi:10.1007/s10596-017-9692-6.
[26] P. Druetta, P. Tesi, C.D. Persis, F. Picchioni, Methods in oil recovery processes and reservoir simulation, Adv. Chem. Eng. Sci. 6 (04) (2016) 39, doi:10.4236/aces.2016.64039.
[27] M.S. Bidner, G.B. Savioli, On the numerical modeling for surfactant flooding of oil reservoirs, Mecanica Computacional XXI (2002) 566–585.
[28] P. Druetta, J. Yue, P. Tesi, C.D. Persis, F. Picchioni, Numerical modeling of a compositional flow for chemical EOR and its stability analysis, Appl. Math. Model. 47 (2017) 141–159, doi:10.1016/j.apm.2017.03.017.
[29] L.P. Dake, Fundamentals of Reservoir Engineering, Elsevier, Amsterdam, the Netherlands, 1978. ISBN 0-444-41830-X.
[30] D.W. Green, G.P. Willhite, Enhanced Oil Recovery, Society of Petroleum Engineers, Richardson, USA, 1998. ISBN 978-1-55563-077-5.
[31] P. Druetta, F. Picchioni, Numerical modeling and validation of a novel 2d compositional flooding simulator using a second-order TVD scheme, Energies 11 (2018) 2280, doi:10.3390/en11092280.
[32] J. Bear, Dynamics of Fluids In Porous Media, American Elsevier Publishing Company, 1972. ISBN 978-0-44400-114-6.
[33] Z. Chen, G. Huan, Y. Ma, Computational Methods for Multiphase Flows in Porous Media, Society for Industrial and Applied Mathematics, 2006, doi:10.1137/1.9780898718942. ISBN 978-0-89871-606-1.
[34] D. Kuzmin, University Erlangen-Nuremberg, Germany (2010).
[35] R.S. Seright, How much polymer should be injected during a polymer flood? review of previous and current practices, SPE J. 22 (1) (2017) 1–18, doi:10.2118/179543-PA.
[36] E. Ahusborde, M.E. Ossmani, A sequential approach for numerical simulation of two-phase multicomponent flow with reactive transport in porous media, Math. Comput. Simulation 137 (2017) 71–89, doi:10.1016/j.matcom.2016.11.007.
[37] J. Bear, Y. Bachmat, Macroscopic modeling of transport phenomena in porous-media .2. applications to mass, momentum and energy-transport, Transp. Porous Media 1 (3) (1986) 241–269, doi:10.1007/BF00238182.
[38] B. Braconnier, C. Preux, E. Flauraud, Q.H. Tran, C. Berthon, An analysis of physical models and numerical schemes for polymer flooding simulations, Comput.l Geosci. 21 (5–6) (2017) 1267–1279, doi:10.1007/s10596-017-9637-0.
[39] D. Camilleri, S. Engelson, L.W. Lake, E.C. Lin, T. Ohnos, G. Pope, K. Sepehrnoori, Description of an improved compositional micellar/polymer simulator, SPE Reserv. Eng. 2 (1987a) 427–432, doi:10.2118/13967-PA.
[40] D. Camilleri, A. Fil, G.A. Pope, B.A. Rouse, K. Sepehrnoori, Comparison of an improved compositional micellar/polymer simulator with laboratory corefloods, SPE Reserv. Eng. 2 (1987b) 441–451, doi:10.2118/12083-PA.
[41] R. Cao, L. Cheng, P. Lian, Flow behavior of viscoelastic polymer solution in porous media, J. Dispers. Sci. Technol. 36 (1) (2015) 41–50, doi:10.1080/01932691.2014.882260.
[42] N.F. Najafabadi, Modeling Chemical EOR Processes Using IMPEC and Fully IMPLICIT Reservoir Simulators, The University of Texas at Austin, USA, 2009.
[43] S.T. Hilden, O. Moyner, K.A. Lie, K. Bao, Multiscale simulation of polymer flooding with shear effects, Transp. Porous Media 113 (1) (2016) 111–135, doi:10.1007/s11242-016-0682-2.
[44] A.N. El-hoshoudy, S.E.M. Desouky, A.M. Al-Sabagh, M.A. Betiha, M.Y. E. kady, S. Mahmoud, Evaluation of solution and rheological properties for hydrophobically associated polyacrylamide copolymer as a promised enhanced oil recovery candidate, Egypt. J. Pet. 26 (3) (2017) 779–785, doi:10.1016/j.ejpe.2016.10.012.
[45] M. Li, M. Xu, M. Lin, Z. Wu, The effect of HPAM on crude oil/water interfacial properties and the stability of crude oil emulsions, J. Dispers. Sci. Technol. 28 (1) (2007) 189–192, doi:10.1080/01932690600992829.
[46] M.A. Bataweel, Enhanced Oil Recovery in High Salinity High Temperature Reservoir by Chemical Flooding, Texas A&M University, USA, 2011.
[47] M. Shen, X. Xu, Y. Wang, Y. Guo, M. Fan, G. Tan, J. Wang, Relationship between the polymer structures and destabilization of polymer-containing water-in-oil emulsions, J. Dispers. Sci. Technol. 28 (8) (2007) 1178–1182.
[48] Z. Ye, G. Guo, H. Chen, Z. Shu, Interaction between aqueous solutions of hydrophobically associating polyacrylamide and dodecyl dimethyl betaine, J. Chem. (2014) 932082, doi:10.1155/2014/932082.
[49] D.A.Z. Wever, F. Picchioni, A.A. Broekhuis, Polymers for enhanced oil recovery: a paradigm for structure-property relationship in aqueous solution, Prog. Polym. Sci. 36 (11) (2011) 1558–1628, doi:10.1016/j.progpolymsci.2011.05.006.
[50] M. Pancharoen, Physical Properties of Associative Polymer Solutions, Stanford University, Stanford, USA, 2009.
[51] M. Lotfollahi, H. Koh, Z. Li, M. Delshad, G.A. Pope, Mechanistic simulation of residual oil saturation in viscoelastic polymer floods, in: SPE EOR Conference at Oil and Gas West Asia, Society of Petroleum Engineers, 2016, doi:10.2118/179844-MS.
[52] J. Wang, H.Q. Liu, J. Xu, Mechanistic simulation studies on viscous-elastic polymer flooding in petroleum reservoirs, J. Dispers. Sci. Technol. 34 (3) (2013) 417–426, doi:10.1080/01932691.2012.660780.
[53] R. Dawson, R.B. Lantz, Inaccessible pore volume in polymer flooding, Soc. Pet. Eng. J. 12 (5) (1972) 448.
[54] J.R. Gilman, D.J. MacMillan, Improved interpretation of the inaccessible pore-volume phenomenon, SPE Form. Eval. 2 (1987) 442–448, doi:10.2118/13499-PA.
[55] W.C. Liauh, J.L. Duda, E.E. Klaus, An investigation of the inaccessible pore volume phenomena, Interfacial Phenom. Enhanc. Oil Recov. 78 (212) (1979) 70–76. SPE-8751-MS.
[56] M. Pancharoen, M.R. Thiele, A.R. Kovscek, Inaccessible pore volume of associative polymer floods, in: SPE Improved Oil Recovery Symposium, Society of Petroleum Engineers, 2010, doi:10.2118/129910-MS
[57] K.S. Lee, Performance of a polymer flood with shear-thinning fluid in heterogeneous layered systems with crossflow, Energies 4 (8) (2011) 1112–1128, doi:10.3390/en4081112.
[58] R. Seright, Use of polymers to recover viscous oil from unconventional reservoirs. final report, 2011, Technical Report, DE-NT0006555, US Department of Energy.
[59] N. Yacob, N. Talip, M. Mahmud, N. Sani, N. Akma, N.A.F. Samsuddin, Determination of viscosity-average molecular weight of chitosan using intrinsic viscosity measurement, J. Nucl. Relat. Technol. 10 (1) (2013) 39–44.

[60] P.J. Flory, Principles of Polymer Chemistry, Cornell University Press, 1953. doi: 978-0-80140-134-3.
[61] A. Gleadall, J. Pan, Computer simulation of polymer chain scission in biodegradable polymers, J. Biotechnol. Biomater. 3 (2013) 154.
[62] A. Gleadall, J. Pan, M.A. Kruft, M. Kellomaki, Degradation mechanisms of bioresorbable polyesters. part 1. effects of random scission, end scission and autocatalysis, Acta Biomater. 10 (5) (2014a) 2223–2232, doi:10.1016/j.actbio.2013.12.039.
[63] A. Gleadall, J. Pan, M.A. Kruft, M. Kellomaki, Degradation mechanisms of bioresorbable polyesters. part 2. effects of initial molecular weight and residual monomer, Acta Biomater. 10 (5) (2014b) 2233–2240, doi:10.1016/j.actbio.2014.01.017.
[64] B. McCoy, G. Madras, Degradation kinetics of polymers in solution: dynamics of molecular weight distributions, AIChE J.l 43 (3) (1997) 802–810, doi:10.1002/aic.690430325.
[65] R. Moreno, A. Muller, A. Saez, Flow-induced degradation of hydrolyzed polyacrylamide in porous media, Polym. Bull. 37 (5) (1996) 663–670, doi:10.1007/BF00296613.
[66] A. Tayal, S. Khan, Degradation of a water-soluble polymer: molecular weight changes and chain scission characteristics, Macromolecules 33 (26) (2000) 9488–9493, doi:10.1021/ma000736g.
[67] M.T. Ghannam, S.W. Hasan, B. Abu-Jdayil, N. Esmail, Rheological properties of heavy & light crude oil mixtures for improving flowability, J. Pet. Sci. Eng. 81 (2012) 122–128, doi:10.1016/j.petrol.2011.12.024.
[68] B. Liang, H. Jiang, J. Li, R.S. Seright, L.W. Lake, Further insights into the mechanism of disproportionate permeability reduction, in: SPE Annual Technical Conference and Exhibition, Society of Petroleum Engineers, 2017, doi:10.2118/187364-MS
[69] R.S. Seright, Optimizing disproportionate permeability reduction, in: SPE/DOE Symposium on Improved Oil Recovery, Society of Petroleum Engineers, 2006, doi:10.2118/99443-MS.
[70] S. Nilsson, A. Stavland, H.C. Jonsbraten, Mechanistic study of disproportionate permeability reduction, in: SPE/DOE Improved Oil Recovery Symposium, Society of Petroleum Engineers, 1998, doi:10.2118/39635-MS.
[71] R. Eymard, C. Guichard, R. Masson, Grid orientation effect in coupled finite volume schemes, IMA J. Numer. Anal. 33 (2013) 582–608, doi:10.1093/imanum/drs016.